Characterisation of cold-selective lamina I spinal projection neurons

Aimi N. Razlan[1,4], Wenhui Ma[1,4], Allen C. Dickie[1,4], Erika Polgár[1,4], Anna McFarlane[1], Mansi Yadav[1], Andrew H. Cooper[1], Douglas Strathdee[2], Masahiko Watanabe[3], Andrew M. Bell[1], Andrew J. Todd[1]*, Junichi Hachisuka[1]*

[1]School of Psychology and Neuroscience, College of Medical, Veterinary and Life Sciences, University of Glasgow, Glasgow G12 8QQ, UK

[2]School of Cancer Sciences, College of Medical, Veterinary and Life Sciences, University of Glasgow, Bearsden G61 1BD UK

[3]Department of Anatomy, Hokkaido University School of Medicine, Sapporo 060-8638, Japan

[4]Equal contribution

*Corresponding Authors: Andrew.Todd@glasgow.ac.uk and Junichi.Hachisuka@Glasgow.ac.uk

Click here to enter text.

ABSTRACT

Skin cooling is detected by primary afferents that express the Trpm8 channel, but how this information is conveyed to the brain remains poorly understood. We have previously identified a population of lamina I projection neurons belonging to the anterolateral system (ALS) that receive numerous contacts from Trpm8-expressing primary afferents. Here, using a semi-intact somatosensory preparation, we show that these cells correspond to the cold-selective ALS neurons identified in previous physiological studies. We also confirm the presence of synapses from Trpm8 afferents onto these cells at the ultrastructural level. Based on our previous transcriptomic findings, we identify calbindin as a molecular marker, and show that this can be used to target the cold-selective ALS neurons for anterograde tracing studies. We provide evidence that they project to 3 brain regions that are associated with thermosensation: the rostralmost part of the lateral parabrachial area, the caudal part of the periaqueductal grey matter, and the ventral posterolateral nucleus of the thalamus. Our findings provide important insights into the organisation of neuronal circuits that underlie thermoregulation and the perception of cold stimuli applied to the skin.

Click here to enter text.

INTRODUCTION

The anterolateral system (ALS) consists of spinal cord neurons that project to various brain regions, including the caudal ventrolateral medulla (CVLM), the nucleus of the solitary tract (NTS), the lateral parabrachial area (LPB), the periaqueductal grey matter (PAG) and the thalamus. ALS neurons are required for the perception of pain, itch and skin temperature, as shown by the loss of these sensations on the side contralateral to an anterolateral cordotomy[1,2]. ALS neurons account for only a small proportion (probably less than 1%) of spinal cord neurons[3,4] and are unevenly distributed, with a relatively high density in lamina I and the lateral spinal nucleus (LSN), and scattered cells in deeper laminae (III-VII) and around the central canal[5-8]. ALS neurons are functionally heterogeneous, and we recently identified 5 distinct transcriptomic populations, which we named ALS1-5[9]. This was based on single-nucleus RNA sequencing of a major subset of these cells, those that transiently express the transcription factor Phox2a during development[10].

Perception of skin cooling is dependent on primary afferent neurons that express the Trpm8 channel[11-15], and these terminate mainly in lamina I of the spinal cord[16-18]. Consistent with this, it has been shown that many lamina I projection neurons respond to cool or cold stimuli applied to the skin, with a distinctive subset of “cold-selective” neurons responding predominantly or exclusively to skin cooling[19-29].

How information is transmitted from Trpm8-expressing primary afferent neurons to these cold-selective lamina I ALS cells is currently not known, although a recent report has suggested that this occurs via a dedicated population of excitatory interneurons[30]. However, we had previously identified a population of lamina I ALS neurons that received dense synaptic input from Trpm8-expressing primary afferents[9]. These neurons had dendrites that were intimately associated with bundles of Trpm8-positive afferents, while their cell bodies generally also received numerous contacts, and were sometimes surrounded by these afferents. We therefore proposed that these cells correspond to the cold-selective neurons described above, and also provided evidence that they belonged to the ALS3 population[9].

The aims of this study were to characterise and validate the Trpm8^{Flp} mouse line that we had used to reveal this input, to confirm the presence of synaptic input at the ultrastructural level, and to test the prediction that the lamina I projection neurons with dense synaptic input from Trpm8-expressing primary afferents do indeed correspond to the cold-selective population described in physiological studies[19-29]. In addition, since

Click here to enter text.

Calb1 (which encodes the calcium-binding protein calbindin) is one of the top differentially expressed genes in the ALS3 population, we used mice in which Cre recombinase is targeted to the Calb1 locus (Calb1^{Cre}) to investigate the projections of the ALS3 cells to the brain.

RESULTS

Validation of Trpm8^{Flp} mouse line and characterisation of Flp-expressing cells.

Trpm8^{Flp} mice were crossed with the Flp reporter line RCE:FRT to generate Trpm8^{Flp};RCE:FRT mice, in which cells that express Flp at any stage during development are labelled with GFP. We used a stereological technique to quantify neurons in an L4 dorsal root ganglion (DRG) from 3 of these mice and found that 5.7% (range 5.4-6.7%) of all DRG neurons contained GFP (Figure 1A). We then performed fluorescence *in situ* hybridisation (FISH) to examine the extent of overlap between GFP and *Trpm8* mRNA (Figure 1B). In DRGs from 3 mice, we found that 92% (88%-98%) of GFP-containing cells had *Trpm8* message, while 83% (80%-86%) of cells with *Trpm8* were GFP-positive. These findings show a high degree of fidelity in the Trpm8^{Flp} line, and are consistent with the reported expression of *Trpm8* mRNA in 5-10% of mouse DRG cells[11]. We also used this tissue to determine the soma size of the GFP-positive cells (Figure 1C), and found that these were small, with a mean diameter of 14.6 µm (± 3.4 µm, SD), showing a very similar size range to that reported for cells captured with a different Trpm8^{Flp} mouse line[31]. Trpm8-positive cells that lacked GFP, as well as the few GFP-labelled cells that lacked *Trpm8* mRNA, showed a similar size distribution.

Transcriptomic studies have demonstrated that Trpm8-expressing primary afferents can co-express certain genes that serve as markers for primary afferent populations, such as Slc17a8 (which encodes Vglut3), Trpv1 and Tac1 (the gene coding for substance P), but lack other neuropeptides such as calcitonin gene-related peptide (CGRP) and somatostatin[32,33]. We therefore performed immunohistochemistry to look for expression of the corresponding proteins/peptides in dorsal root ganglia from 3 mice in each case. We found that 11.9% (9.8-13.8%) of GFP-containing cells were immunoreactive for Vglut3 and 26.4% (22.4-30.9%) for Trpv1 (Figure 1–figure supplement 1A-D). Among the neuropeptides, we found minimal co-localisation with CGRP (mean 2.5%, range 1.4-4.5%) and none with somatostatin. However, 56% (range 55.8-56.3%) of the GFP cells contained substance P, although this was expressed at relatively low levels (Figure 1–figure

Click here to enter text.

supplement 1G-M). These results are therefore consistent with the transcriptomic findings described above[32,33].

Central projections of Trpm8-expressing primary afferents have been shown to terminate mainly in lamina I[16-18], and we found a similar pattern in the spinal cords of Trpm8^{Flp};RCE:FRT mice, with the great majority of GFP-labelled axons remaining in lamina I, and very few passing ventrally (Figure 2). We had previously noted that when lamina I was viewed in horizontal sections, Trpm8 afferents were arranged in interweaving bundles that frequently followed the dendrites of a distinctive subset of projection neurons[9]. Consistent with this, we found that Trpm8 afferents showed a discontinuous arrangement within lamina I when viewed in transverse sections and did not occupy the whole medio-lateral extent of the lamina (Figure 2).

It has been reported that some lamina I projection neurons were associated with boutons that were immunoreactive for Vglut3[34] and since 12% of Trpm8 afferent cell bodies contained Vglut3, we looked for expression of the transporter in their central terminals. In transverse sections, Vglut3-immunoreactive axons formed a dense band in inner lamina II that corresponds to central terminals of C-low threshold mechanoreceptors (C-LTMRs)[35,36]. However, there were a few Vglut3-immunoreactive boutons in lamina I that were also GFP-positive, indicating that central terminals of some Trpm8-expresing primary afferents had detectable levels of the transporter (Figure 2–figure supplement 1A-F). We generated a mouse genetic cross (Phox2a::Cre;Ai9;Trpm8^{Flp};RCE:FRT) in which a subset of ALS cells express tdTomato and Trpm8 afferents express GFP. In horizontal sections from these mice we identified lamina I projection neurons that were associated with numerous GFP-labelled (Trpm8-expressing) boutons and found that some of these boutons contained Vglut3 (Figure 2–figure supplement 1G-J). Since C-LTMRs do not appear to arborise in lamina I[31], it is likely that the Vglut3-containing boutons that have been found to contact projection neurons in this lamina[34] belong to Trpm8 afferents. Although many Trpm8-positive cell bodies showed Trpv1 and substance P immunoreactivities, we were not able to detect either of these in their central terminals.

Synaptic input from Trpm8-expressing afferents to lamina I projection neurons.

We had previously shown that ~20% of lamina I projection neurons retrogradely labelled from the LPB received numerous contacts from GFP-labelled afferents in Trpm8^{Flp};RCE:FRT mice, and that these contacts were associated with punctate staining for Homer1[9] (a marker for glutamatergic synapses[37]). To reveal synapses formed between

Click here to enter text.

135 Trpm8 afferents and these projection neurons at the ultrastructural level, we used a
136 combined confocal/electron microscopic method[38] on spinal cord tissue from
137 Phox2a::Cre;Ai9;Trpm8^{Flp};RCE:FRT mice. This genetic cross was chosen because we had
138 previously shown that the Phox2a-lineage includes many lamina I ALS neurons with dense
139 input from Trpm8 afferents[9]. Horizontal sections from lumbar spinal cord segments of 2 of
140 these mice were immunostained to reveal tdTomato and GFP, and 3 tdTomato-labelled
141 cells with numerous contacts from GFP-labelled axons were scanned with a confocal
142 microscope (Figure 3, Figure 3–figure supplements 1 and 2). The tissue was subsequently
143 processed with an immunoperoxidase method to label the GFP-positive axons with
144 diaminobenzidine (DAB), and examined with an electron microscope (Figure 3, Figure 3–
145 figure supplement 2). Although the cell bodies and dendrites of the projection neurons did
146 not contain an electron-dense label, they could be readily identified by their location within
147 the ultrathin sections, by their association with numerous DAB-labelled axonal boutons
148 and by the morphology of their somata and proximal dendrites (Figure 3A,B). Because of
149 the very high density of GFP-labelled boutons that were seen to contact the cells in the
150 confocal images, it was not always possible to relate individual boutons from confocal
151 images to those seen with the electron microscope. However, we were able to identify
152 numerous axosomatic and axodendritic synapses (a minimum of 10 synapses per cell)
153 between the GFP-immunoreactive boutons and the lamina I projection neurons. These
154 could be recognised by the presence of darkening of the membranes and in some cases a
155 faint postsynaptic density, together with clustering of synaptic vesicles on the presynaptic
156 side (Figure 3B-D, Figure 3–figure supplement 2C-J). Interestingly, the synapses between
157 the GFP-containing boutons and the projection neurons generally had relatively faint
158 postsynaptic densities and only small regions where the vesicles were clustered on the
159 presynaptic side. These findings, together with our previous observation of Homer1-
160 immunoreactive puncta located between GFP-expressing afferent boutons and the cell
161 bodies and dendrites of retrogradely labelled lamina I projection neurons in
162 Trpm8^{Flp};RCE:FRT mice[9], indicate that ALS cells belonging to this population receive
163 numerous synapses from Trpm8-expressing primary afferents.
164

165 **Lamina I ALS neurons that are surrounded by Trpm8 afferents are cold-selective**

166 We next tested whether the lamina I projection neurons that are densely innervated by
167 Trpm8 afferents correspond to the cold-selective neurons identified in physiological
168 studies[19-29]. To do this, we carried out whole-cell patch-clamp recordings in preparations in

Click here to enter text.

169 which ALS neurons were retrogradely labelled with either mCherry or tdTomato, and
170 Trpm8 axons expressed GFP. We used the semi-intact *ex vivo* somatosensory
171 preparation, in which the spinal cord, L2 and L3 roots and ganglia, saphenous and femoral
172 cutaneous nerves, and hindlimb skin are dissected in continuity[25].

173 Visualisation of the spinal cord with filter sets for GFP or mCherry/tdTomato revealed
174 lamina I projection neurons (labelled with mCherry or tdTomato) as well as a plexus of
175 GFP-labelled (Trpm8-expressing) primary afferents (Figure 4). We recorded from 6
176 mCherry/tdTomato-labeled projection neurons that had dendrites (and in some cases also
177 cell bodies) that were clearly associated with numerous GFP-labelled afferents, as well as
178 from 5 projection neurons for which there was no clear association with these afferents.
179 We assessed the responses of these cells to a 4 g von Frey filament, hot saline, and cold
180 saline applied to the skin[27]. All 6 of the projection neurons that had numerous contacts
181 from GFP-labelled axons responded exclusively to application of cold saline. In 4 cases
182 recordings were made in current clamp and the cells fired action potentials (n = 3) or
183 generated EPSPs (subthreshold, n = 1) following application of cold saline, but showed no
184 response to mechanical or heat stimuli (Figure 4). The time course of the response was
185 consistent with that seen for cold-selective projection neurons that we previously reported
186 (Figure 4–figure supplement 1)[28]. The other two cells with numerous GFP contacts were
187 recorded in voltage clamp, and these showed EPSCs in response to cold, but not
188 mechanical or heat, stimuli. All six of these neurons were therefore classified as cold-
189 selective. The five projection neurons that were not preferentially associated with GFP-
190 labelled afferents were all recorded in current clamp mode, and all of these cells exhibited
191 action potential firing in response to mechanical stimulation. Three of them also responded
192 to heat, and one additionally to cold stimuli. The five neurons that were not associated with
193 numerous GFP-labelled afferents were therefore classified as either mechano-selective or
194 polymodal (Figure 4).

195 We previously reported that cold-selective projection neurons are distinct from other
196 lamina I projection neurons[28], and a defining feature of these cells was their low frequency
197 of spontaneous EPSCs (sEPSCs). We therefore quantified sEPSC frequency and
198 amplitude in lamina I projection neurons with or without dense Trpm8 input. As expected,
199 neurons with dense Trpm8 input had significantly lower sEPSC frequencies compared to
200 those that lacked dense Trpm8 input (Figure 4–figure supplement 1). Interestingly, the
201 amplitude of sEPSCs in the projection neurons with dense Trpm8 input was smaller than
202 in those that lacked this input, which had not been observed in our previous study[28].

Click here to enter text.

Together, these results demonstrate that lamina I projection neurons receiving dense Trpm8 afferent innervation constitute a distinct neuronal population specialised for cold sensation, and correspond to the cold-selective ALS neurons identified in previous studies[19-29].

Our anatomical studies indicate that the cells densely coated with Trpm8-expressing primary afferents receive many synapses from these afferents (Figure 3), and we had shown previously that these cells had numerous Homer1-immunoreactive puncta, with ~60% being associated with a Trpm8-expressing primary afferent bouton[9]. The low frequency of sEPSCs is therefore not likely to result from a low density of synapses, but presumably reflects a very low release probability at these synapses in these experimental conditions. The lower amplitude of sEPSCs may be related to our EM observation that contacts between Trpm8 afferents and densely coated lamina I projection neurons typically have small synaptic specialisations (Figure 3, Figure 3–figure supplement 2).

Targeting of cold-selective lamina I ALS neurons with the Calb1^{Cre} mouse

We had previously demonstrated that lamina I projection neurons that are densely innervated by Trpm8-expressing afferents are included among those of the Phox2a-lineage, and contain mRNA for *Hs3st1*, one of the top differentially expressed genes for ALS3. We had therefore assigned the Trpm8-innervated cells to the ALS3 cluster[9]. Calb1, which encodes the calcium-binding protein calbindin, is also among the top 20 differentially expressed genes for ALS3 (Figure 5–figure supplement 1A, see also Figure 1D of reference[9]). However, calbindin is not restricted to the ALS3 cluster, as it is also expressed by some cells in the ALS2, ALS4 and ALS5 clusters[9] (Figure 5–figure supplement 1A), and by many ALS neurons in the lateral spinal nucleus (LSN)[39], most of which are not derived from the Phox2a-lineage[10,40].

To assess the relationship between Calb1-expressing ALS neurons and those with dense Trpm8 innervation, we injected an AAV coding for Cre-dependent tdTomato (AAV11.Cre^{ON}.tdTomato) unilaterally into the LPB of 4 Calb1^{Cre};Trpm8^{Flp};RCE:FRT mice (Figure 5–figure supplement 1B). As expected from the known distribution of calbindin-expressing ALS cells in the rat[39], we observed tdTomato-positive cells in lamina I (mainly on the contralateral side), as well as bilaterally in the LSN and in deeper laminae (Figure 5A, Figure 5–figure supplement 1C-F). When we examined horizontal sections through lamina I, we found that many of the tdTomato-labelled cells, were densely innervated by Trpm8 afferents (Figure 5C-H). The proportion of tdTomato cells with dense Trpm8 input

Click here to enter text.

varied between 38.7-59.6% across the L2-L4 segments (Figure 5B, RM ANOVA, p = 0.048). Interestingly, the proportion was significantly higher in L2 (59.6%) than in L4 (38.7%), (RM ANOVA, Holm-Šídák's multiple comparisons test, p = 0.0056, n = 4), and this may reflect a difference in the proportion of lamina I cells with dense Trpm8 innervation between segments. When results across the 3 segments were pooled, the total numbers of retrogradely labelled cells ranged from 133 to 170 (mean 151), while the proportions ranged from 46.5%-54.1% (mean 50.6%). We also used the semi-intact preparation to record from tdTomato-labelled lamina I neurons in spinal cords from 4 Calb1^{Cre} mice that had received injections of AAV11.Cre^{ON}.tdTomato into the CVLM (Figure 5–figure supplement 1B,G-I). We recorded from 6 retrogradely labelled neurons and found that 5 were cold-selective, while one was polymodal, responding to brushing of the skin, as well as to application of both hot and cold stimuli (Figure 5I,J). These cold-selective neurons showed a similar time course in response to cold stimulation to those described above (Figure 5–figure supplement 1I). Taken together, these findings indicate that while Calb1 is not restricted to cold-selective cells, many of the Calb1-expressing projection neurons in lamina I belong to the cold-selective population.

Brain projections of putative cold-selective lamina I neurons

Because Calb1 is expressed by cold-selective ALS cells in lamina I, we carried out anterograde tracing by injecting AAV coding for Cre-dependent expression of tdTomato (AAV1.Cre^{ON}.tdTom) into the spinal cords of Calb1^{Cre} mice. Our aim was to test for projections to two potential brainstem targets that receive input from the ALS[7,8] and also contain many neurons that express the immediate early gene Fos in mice exposed to low ambient temperatures[41-44]: the caudal part of the PAG (cPAG), and the rostral part of the LPB, in particular a region that has been named PBrel (rostral to external lateral)[42]. In addition, we looked for evidence of an input to the ventral posterolateral (VPL) nucleus of the thalamus, which through its connections with the primary somatosensory (S1) cortex, could underlie the conscious perception of skin cooling. Initially, we examined labelling resulting from injections of AAV1.Cre^{ON}.tdTomato that were targeted on the central part of the dorsal horn, either in the L3 segment, or in the L3, L4 and L5 segments, using a similar approach to that which we had taken with other genotypes[45,46] (Figure 6–figure supplement 1A,B; Table 1). Labelling patterns were consistent among the mice used in this part of the study, but labelling was denser in all regions in those that had received injections into L3, L4 and L5. This approach revealed that axons ascended in the

Click here to enter text.

271 dorsolateral white matter of the spinal cord and gave branches to several regions on the
272 contralateral side of the brainstem, including LPB and the cPAG (Figure 6–figure
273 supplement 1C,D). Within the LPB, axonal labelling was very dense in the rostral-most
274 part, which corresponds to PBrel[42], and moderately dense in the centrolateral (PBcl)
275 nucleus. In addition, there was some labelling in other nuclei, including external lateral
276 (PBel), dorsolateral (PBdl) and internal lateral (PBil). There was dense labelling in the
277 cPAG and in addition, labelling was seen within the superior colliculus (Figure 6–figure
278 supplement 1C). In the thalamus, there was sparse labelling in the VPL and posterior (Po)
279 nuclei contralateral to the injection site, and many labelled profiles were present in the
280 medial thalamus on both sides (Figure 6–figure supplement 1E). These findings were
281 therefore consistent with the expected projections of cold-selective ALS cells to PBrel,
282 cPAG and the VPL nucleus of thalamus.

283 However, this strategy will also have labelled Calb1-expressing projection neurons in
284 other regions, including the LSN and the lateral reticulated part of lamina V (Figure 6–
285 figure supplement 1B). Consistent with this interpretation, we observed labelling in PBil
286 and the medial thalamus, both of which are known to receive input from ALS cells in the
287 deep dorsal horn[47-49], including cells belonging to the ALS4 population in lateral lamina
288 V[45]. We therefore altered the injection technique by reducing the volume and injecting at a
289 more medial location (250 μm rather than 400 μm lateral to the midline). As with the
290 previous experiments, these injections were either made into the L3 segment, or into each
291 of L3, L4 and L5 (Table 1). Again, the pattern of labelling was consistent among these
292 mice, but labelling was denser in those that had received injections into L3, L4 and L5.
293 This strategy resulted in injection sites that were restricted to the medial part of the dorsal
294 horn and excluded the LSN (Fig 6A-C). Although very weak tdTomato labelling was seen
295 in the LSN in these experiments, this is likely to have arisen from transport by axons of
296 local calbindin-expressing excitatory interneurons, since many excitatory interneurons in
297 laminae I-II have axons that enter the LSN[50-52]. Importantly, no tdTomato-labelled cell
298 bodies were seen in the LSN or in the lateral reticulated part of lamina V in these cases.
299 Since these injections were likely to have included a much higher proportion of lamina I
300 neurons with dense Trpm8 innervation, we analysed the anterograde labelling in more
301 detail.

302 Axons ascended in the dorsal quadrant of the spinal cord, mainly on the contralateral
303 side (Figure 6–figure supplement 2A). Although a few collaterals arose at all segmental
304 levels examined, these were far less numerous than those originating from the

Click here to enter text.

305 somatostatin-expressing ALS cells that occupy the lateral part of lamina V[45]. Ascending
306 axons lay near the ventrolateral surface of the medulla, and sent collateral branches to the
307 NTS (Figure 6D), but unlike Gpr83- and Tacr1-expressing ALS cells[45,53], these Calb1-
308 positive cells did not innervate the inferior olive. Labelling in the LPB was much more
309 restricted following medial spinal injections, compared to the central injections (Figure 6E,
310 Figure 6–figure supplement 1C,D, Figure 6–figure supplement 2B). In particular, labelling
311 in PBcl and PBil was greatly reduced, while the dense input to the PBrel was retained. The
312 input to PBrel was confirmed by immunostaining for the transcription factor Foxp2, which is
313 expressed in PBrel neurons (Fig 6G,H)[42]. There was also strong labelling in the lateral part
314 of the cPAG, (Figure 6E), but only very sparse labelling in the rostral part of the PAG
315 (Figure 6–figure supplement 2C,E). Input to both LPB and PAG was bilateral, but denser
316 on the side contralateral to the spinal injections. Labelling in the superior colliculus was
317 almost completely lost following medial spinal injections (Figure 6E). Within the thalamus,
318 the sparse labelling in VPL and Po was still present, but that in the medial thalamus was
319 far weaker (Figure 6F,I,J). In addition, medial spinal injections resulted in some labelling in
320 the posterior triangular (PoT) nucleus of the thalamus, which is a known target for lamina I
321 ALS neurons[49,54] (Figure 6–figure supplement 2C,D). Very few, if any, tdTomato-labelled
322 axons were seen in any other parts of the diencephalon[55].
323 The differences between projection patterns of medial and central intraspinal injections
324 provide additional information about potential targets of Calb1 cells that were not located in
325 lamina I. As noted above, the input to PBil and medial thalamus seen following the central
326 injections is likely to result at least in part from capture of cells belonging to the ALS4
327 population in lateral lamina V[9], since we have shown that these cells (targeted in a Sst^{Cre}
328 mouse line) project to these two sites[45]. However, we found only very sparse input from
329 the Sst-expressing (ALS4) cells to the superior colliculus[45], raising the possibility that input
330 to the colliculus originates mainly from cells in the LSN, many of which express Calb1.
331 Consistent with this suggestion, Choi et al[53] observed a projection to the superior colliculus
332 from Tacr1-expressing ALS cells, and many ALS neurons in the LSN express the
333 neurokinin 1 receptor (NK1r), which is encoded by Tacr1[46,56,57].
334 To confirm the input to PAG from cold-selective lamina I cells, we targeted injections of
335 AAV11.Cre^{ON}.tdTomato to the caudal PAG in 3 Calb1^{Cre};Trpm8^{Flp};RCE:FRT mice. In these
336 experiments, the total numbers of retrogradely labelled (tdTomato-positive) lamina I cells
337 in the L2-L4 segments were lower than was the case for the LPB injection experiments
338 (26, 59 and 99 in the three cases), but the proportion of these cells that had dense Trpm8

Click here to enter text.

339 input was significantly higher: 84.6%, 81.4% and 77.8% ($p < 0.0001$, unpaired t-test with
340 Welch's correction; Figure 6–figure supplement 3). This indicates that, at least for
341 calbindin-expressing lamina I ALS neurons, cold-selective cells are highly enriched among
342 those that project to the caudal part of the PAG.
343 Finally, we looked for further evidence of a projection from cold-selective lamina I cells
344 to the lateral part of the thalamus by making small injections of cholera toxin B subunit
345 (CTB) in 3 Trpm8^{Flp};RCE:FRT mice. CTB was used as a retrograde tracer for these
346 experiments, because it can result in relatively small and well-defined injection sites. In all
347 3 cases, the injection was centred on the ventral posterior nucleus of thalamus, and
348 included both lateral (VPL) and medial (VPM) parts (Figure 6–figure supplement 4A-C).
349 There was some spread into Po and the ventrolateral (VL) nucleus, but none into the
350 medial thalamus and none of the injections extended as far caudally as the PoT. We have
351 previously demonstrated that although spinothalamic lamina I neurons are relatively
352 common in the rodent cervical enlargement, they are far less numerous at lumbar levels,
353 accounting for <5% of lamina I ALS neurons[40,58]. As expected, few (if any) retrogradely
354 labelled cells were seen in the lumbar spinal cord in these experiments (5 cells in the L4
355 segment of one mouse, but no cells in this segment in the other two), and for this reason
356 we focused our search on the cervical enlargement. In horizontal sections through the C7
357 segment, we identified many retrogradely labelled lamina I cells in each case. Although the
358 dendritic filling was less complete than that seen with retrograde viral tracing, we were
359 able to identify CTB-positive cells that received numerous contacts on cell bodies and
360 dendrites from Trpm8-expressing primary afferents (Figure 6–figure supplement 4D-I). In
361 the one case in which retrogradely labelled cells were detected in the L4 segment, 3 of the
362 5 cells were also densely coated with GFP-labelled afferents (Figure 6–figure supplement
363 4J-L). These findings demonstrate that cold-selective lamina I ALS neurons project to the
364 lateral thalamus.
365
366 **DISCUSSION**
367 The main findings of this study are that: (1) lamina I projection neurons that are densely
368 innervated by Trpm8-expressing primary afferents correspond to the cold-selective cells
369 identified in physiological studies; (2) these are captured when AAVs encoding Cre-
370 dependent constructs are injected into the brains of Calb1^{Cre} mice; and (3) axons of Calb1-
371 positive neurons in the medial part of the dorsal horn project to three brain regions known
372 to be involved in processing information related to cold input, PBrel, caudal PAG and

Click here to enter text.

373 lateral thalamus, suggesting that these sites are directly innervated by cold-selective ALS
374 neurons.
375
376 **Lamina I ALS neurons with dense Trpm8 input are cold-selective**
377 We had previously observed that Trpm8-expressing primary afferents are closely
378 associated with the cell bodies and dendrites of a subset of ALS cells in lamina I[9]. Based
379 on their association with Homer1 puncta, we were also able to estimate that GFP-labelled
380 (Trpm8-expressing) afferents accounted for ~60% of the excitatory synapses on these
381 ALS cells. Here we directly demonstrate the presence of synapses with electron
382 microscopy, and confirm our prediction[9] that these densely Trpm8-innervated ALS cells
383 correspond to the cold-selective neurons identified in previous physiological studies[19-29].
384 Cold-selective lamina I projection neurons have been reported in several species,
385 including monkey[23], cat[19-22], rat[24,26] and mouse[25,27-29], and a recent *in vivo* calcium-imaging
386 study reported that they accounted for ~15% of lamina I spinoparabrachial neurons in the
387 mouse[29]. Although cold-selective lamina I projection neurons respond predominantly to
388 skin cooling, some show a weak "paradoxical" response when noxious heat is applied to
389 the skin[20,22,23,25]. We did not detect any response from cold-selective cells when hot saline
390 was applied to the skin in the experiments reported here, or in our previous study of cold-
391 selective neurons[28], and this may be because although the temperature of the hot saline
392 was 50°C, the small volume applied to the skin meant that skin temperature did not reach
393 a sufficiently high level to result in activation. It is known that some Trpm8-expressing
394 primary afferents have low levels of Trpv1[16,31,33], and some Trpm8 afferents have been
395 shown to respond weakly to noxious heat *in vivo*[31]. It has been proposed that there are two
396 different populations of Trpm8-expressing afferents: one consisting of cells that lack Trpv1
397 and respond to innocuous cooling, and the other of cells that express Trpv1, and may
398 function as "cold nociceptors"[59]. Since we found Trpv1-immunoreactivity in around a
399 quarter of GFP-labelled dorsal root ganglion cells, it is likely that both populations are
400 included amongst the GFP-expressing cells in the Trpm8^{Flp};RCE:FRT mice. However, we
401 were unable to detect Trpv1-immunoreactivity in the central terminals of any GFP-positive
402 axons (presumably reflecting the low level of Trpv1 expressed by these cells), and we
403 therefore do not know whether the Trpm8-positive axons synapsing on cold-selective
404 lamina I ALS neurons include those that express Trpv1. However, if this is the case, it is
405 likely to explain the weak response to noxious heat reported for some cold-selective
406 projection neurons[20,22,23,25].

Click here to enter text.

407

408 **Direct and indirect input from Trpm8 afferents to cold-selective ALS neurons**

409 Our findings clearly demonstrate a major direct (monosynaptic) input from Trpm8-
410 expressing primary afferents to cold-selective lamina I projection neurons. We had
411 previously estimated that a mean of 62% of the Homer1 puncta (which correspond to
412 excitatory synapses) on cell bodies and dendrites of these cells were associated with
413 GFP-positive boutons in Trpm8^{Flp}:RCE:FRT mice[9]. However, we show here that this line
414 only labels ~83% of Trpm8-expressing primary afferent neurons with GFP. If this
415 proportion applies equally to Trpm8 afferents that synapse on cold-selective ALS cells,
416 then Trpm8 afferents would give rise to ~75% of the excitatory synapses on these cells.

417 Lee et al[30] recently proposed that there is a dedicated population of superficial dorsal
418 horn excitatory interneurons that express the thyrotropin releasing hormone receptor (Trhr)
419 and form a disynaptic link between Trpm8 afferents and cold-selective lamina I projection
420 neurons. Interestingly, in their initial experiments, they ablated or silenced calbindin-
421 expressing dorsal horn neurons and found that this reduced behavioural responses to skin
422 cooling. Although they interpreted this as resulting from loss of function of calbindin-
423 expressing excitatory interneurons, our findings indicate that they are also likely to have
424 ablated or silenced calbindin-expressing cold-selective lamina I ALS neurons. This could
425 therefore have made a major contribution to the reduced sensitivity to skin cooling. Having
426 obtained evidence that cold-responsive Calb1+ neurons in the dorsal horn often co-
427 expressed Trhr, Lee et al generated a Trhr^{Cre} mouse line and used spinal injection of AAVs
428 coding for Cre-dependent constructs, or a genetic intersectional approach, to target Trhr-
429 expressing spinal neurons[30]. They ablated these cells and found that this selectively
430 reduced responses to skin cooling. They also reported that when AAV.Cre^{ON}.YFP was
431 injected intraspinally in Trhr^{Cre} mice, there was no axonal labelling in the brain, suggesting
432 that Trhr-expressing dorsal horn neurons were exclusively interneurons. However, this
433 observation is not consistent with our transcriptomic dataset[9], which reveals Trhr
434 expression in some Phox2a-derived ALS neurons, including some of those in the ALS3
435 cluster (Figure 7-figure supplement 1). It is therefore not clear why a brain projection from
436 Trhr cells was not detected by Lee et al, although it is possible that the survival time
437 allowed for anterograde transport of YFP (reported as 2-3 weeks) was not sufficient. Lee
438 et al[30] also reported that the cold-selective ALS neurons were marked by expression of the
439 calcitonin receptor-like receptor (encoded by the *Calcrl* gene). However, this is unlikely to
440 be a specific marker, as our data show expression of Calcrl among several populations of

Click here to enter text.

441 Phox2a-derived ALS neurons[9] (Figure 7-figure supplement 1), and it has been reported
442 that Calcrl is also expressed by spinoparabrachial neurons that are required for
443 mechanical itch[60].
444 While our findings do not exclude the possibility that there is a specific population of
445 interneurons that link Trpm8-expressing primary afferents to cold-selective ALS neurons in
446 lamina I, they clearly demonstrate a substantial direct (monosynaptic) input from Trpm8
447 afferents to cold-selective lamina I projection neurons, and indicate the need for caution in
448 relying on the specificity of individual genetic markers to define neurons and circuits in the
449 dorsal horn.
450
451 **Brain targets of cold-selective ALS cells**
452 At present there is no known molecular marker that could be used to target cold-
453 selective lamina I ALS cells exclusively. We chose calbindin because *Calb1* is among the
454 top differentially expressed genes in the ALS3 cluster[9], and there is a well-established
455 knock-in Cre line available[61]. Importantly, our transcriptomic analysis[9] was restricted to
456 projection neurons derived from the Phox2a lineage[10], which excludes most ALS cells in
457 the LSN and ~40% of those in lamina I[10,40]. Menetrey et al[39] had demonstrated that
458 calbindin-immunoreactive spinoparabrachial neurons in rat were located in lamina I, the
459 LSN and lateral lamina V, with scattered cells around the central canal, and this closely
460 matches the distribution of cells labelled when AAV11.Cre^{ON}.tdTomato was injected into
461 the LPB of Calb1^{Cre} mice. For anterograde tracing, we were able to exclude LSN and
462 lateral lamina V ALS cells by injecting smaller volumes into the medial part of the dorsal
463 horn, and this was confirmed by the lack of axonal labelling in regions known to receive
464 input from these cells (e.g., PBil and medial thalamus)[45,47,49]. However, although our
465 medial injections preferentially captured cold-selective lamina I ALS neurons they will also
466 have labelled cells that are not cold-selective, including some lamina I cells in the ALS2
467 cluster[9] and potentially some of those that are not derived from the Phox2a lineage[40]. We
468 therefore focused our analysis on brain regions known to be involved in cold sensing, and
469 tested whether these received input from the Calb1-positive ALS cells.
470 Among the ALS projection targets that contain cells responding to cold, we were able to
471 show a dense input to the rostral part of the LPB and to the cPAG. Two studies have
472 mapped neurons in LPB that express Fos in mice exposed to low ambient
473 temperatures[42,43], and both found that Fos-positive cells were concentrated in the rostral
474 part of the LPB, corresponding to a level ~4.9 mm caudal to bregma (or 1.1 mm caudal to

475 the interaural line)[55]. Yang et al[43] identified the region containing Fos+ cells as part of the
476 external lateral (PBel) nucleus, while Geerling et al[42] defined it as the PBrel, and showed
477 that this area could be recognised by the expression of Foxp2. Yang et al[43] reported that
478 cold-activated cells in this region projected to the preoptic area (POA), which is known to
479 form part of a cold-defence circuit[62], as well as to the dorsomedial hypothalamus (DMH).
480 They also showed that parabrachial neurons targeting DMH promoted activation of brown
481 adipose tissue, suggesting a role for both of these hypothalamic areas in maintenance of
482 body temperature in cold conditions. The cold-selective lamina I ALS cells are therefore
483 likely to provide an important source of input to POA and DMH via their projection to PBrel,
484 thus forming part of the afferent limb of a cold defence pathway (Figure 7).
485 Neurons in the cPAG show increased Fos expression in rats exposed to low ambient
486 temperatures[41], and this region receives an input from cold-activated cells in the
487 hypothalamus[44]. Our results demonstrate that Calb1-positive neurons in the dorsal horn
488 also provide a dense input to the cPAG. Although we cannot be certain that this originates
489 from the cold-selective ALS neurons, there are two lines of evidence to support this
490 suggestion. First, Li et al[63] demonstrated innervation of mouse lamina I spino-PAG
491 neurons by Trpm8-expressing primary afferents, and second, we found that ~80% of
492 Calb1 neurons retrogradely labelled from cPAG received dense Trpm8 input. Consistent
493 with this interpretation, we had previously reported that rat lamina I neurons retrogradely
494 labelled from the PAG seldom showed strong expression of the NK1r, unlike those labelled
495 from the LPB or CVLM[64], and cold-selective lamina I neurons have been shown to respond
496 weakly, if at all, to substance P, the main ligand for this receptor[28]. These findings suggest
497 that the cold-selective lamina I neurons provide a direct input to cPAG, which presumably
498 contributes to the responsiveness of neurons in this region to cooling[41]. Activation of
499 neurons in the cPAG results in brown adipose tissue thermogenesis[65], suggesting a role in
500 maintenance of body temperature in cold conditions (Figure 7).
501 Our CTB injections into the lateral thalamus were centred on the ventral posterior
502 nucleus, with a varying degree of spread into Po, which was also found to receive input
503 from Calb1-positive ALS neurons. It is not possible to determine precisely the region(s)
504 from which retrograde transport would occur, but since we identified lamina I cells in the
505 C7 segment (and in one case also in the L4 segment) with relatively strong CTB labelling
506 that were associated with GFP-labelled axons, these are likely to have projected to the
507 core of the injection site, i.e. the ventral posterior nucleus. As noted above, spinothalamic
508 lamina I neurons are infrequent in the rodent lumbar enlargement[40,58], and this presumably

Click here to enter text.

accounts for the very sparse labelling in VPL that we saw following injections of AAV1.Cre^{ON}.tdTomato into the lumbar spinal cord. However, our findings from the retrograde tracing experiments suggest that cold-selective cells project to VPL, and this is consistent with the demonstration of input from cervical lamina I neurons to VPL in the rat[49]. This pathway, through its link to the somatosensory cortex, is thought to underlie the perception of cold stimuli applied to the skin[66] (Figure 7).

MATERIALS AND METHODS

Key resources table

Reagent or resource	Source	Identifier
Mouse lines		
Trpm8^{Flp}	Dr Mark Hoon	N/A
B6.Cg-Gt(ROSA)26Sor$^{tm9(CAG\text{-}tdTomato)Hze}$/J (Ai9)	Prof. Hongkui Zheng; available from The Jackson Laboratory, ME, USA	Cat#: 007909 RRID: IMSR_JAX:007909
Phox2a::Cre	Prof Artur Kania	N/A
STOCK *Gt(ROSA)26Sor$^{tm1.2(CAG\text{-}EGFP)Fsh}$*/Mmjax (RCE:FRT)	The Jackson Laboratory, ME, USA	Cat#: 032038 RRID:MMRRC_032038-JAX
B6;129S-*Calb1$^{tm2.1(cre)Hze}$*/J (Calb1^{Cre})	The Jackson Laboratory, ME, USA	Cat#: 028532 RRID:IMSR_JAX:028532
AAV constructs		
pENN.AAV.CB7.CI.mCherry.WPRE.RBG (AAV9.mCherry)	Penn Vector Core, PA, USA; available from Addgene, MA, USA	Cat#: 105544-AAV9 RRID:Addgene_105544
pssAAV-2-CAG-EGFP_Cre-WPRE-SV40p(A) (AAV9.EGFP_Cre)	Viral Vector Facility, University of Zurich, Switzerland	Cat#: v25-9
pssAAV-2-CAG-dlox-tdTomato(rev)-dlox-WPRE-bGHp(A) (AAV1.Cre^{ON}.tdTomato)	Viral Vector Facility, University of Zurich, Switzerland	Cat#: v167-1
AAV11.Cre^{ON}.tdTomato	BrainCase Biotechnology Co Ltd, Wuhan, China	Cat#: BC-0870
Antibodies		
Chicken anti-GFP (1:1000)	Abcam plc	Cat#: ab13970 RRID: AB_300798
Rabbit anti-GFP (1:1000)	M Watanabe	RRID:AB_2571573
Rat anti-mCherry (1:1000)	Thermo Fisher Scientific	Cat#: M11217 RRID: AB_2536611
Guinea pig anti-NeuN (1:1000)	Synaptic Systems	Cat#: 266 004 RRID:AB_2619988
Rabbit anti-NeuN-Alexa Fluor® 647 (1:1000)	Abcam plc	Cat#: EPR12763 RRID:AB_2532109

Click here to enter text.

Rat anti-substance P (1:200)	Oxford biotechnology	Cat#: OBT06435
Rabbit anti-substance P (1:1000)	Peninsula	Cat#: T-4107 RRID:AB_518630
Rabbit anti-TRPV1 (1:1000)	Synaptic Systems	Cat#: 444 013 RRID:AB_2864792
Sheep anti-CGRP (1:2000)	Enzo	Cat#: BML-CA1137 RRID:AB_2243859
Rabbit anti-somatostatin (1:500)	Peninsula	Cat#: T-4103 RRID:AB_518614
Guinea pig anti-VGLUT3 (1:100)	M Watanabe	RRID:AB_2571856
Sheep anti-Foxp2 (1:500)	Biotechne	Cat#: AF5647 RRID:AB_2107133
Goat anti-cholera toxin B subunit (1:2000 for immunofluorescence; 1:100,000 for immunoperoxidase)	List Biological	Cat#: 703 RRID:AB_10013220
Alexa Fluor™ Plus 405 Donkey anti-Rabbit IgG (1:500)	Thermo-Fisher Scientific	Cat#: A48258 RRID: AB_2890547
Alexa Fluor® 488 Donkey Anti-Chicken IgY (1:500)	Jackson ImmunoResearch	Cat#: 703-545-155 RRID: AB_2340375
Alexa Fluor® 488 Donkey anti-Goat IgG (1:500)	Jackson ImmunoResearch	Cat#: 705-545-147 RRID: AB_2336933
Alexa Fluor® 488 Donkey Anti-Rabbit IgG (1:500)	Jackson ImmunoResearch	Cat#: 711-545-152 RRID: AB_2313584
Alexa Fluor™ Plus 488 Donkey anti-Rabbit IgG (1:500)	Thermo-Fisher Scientific	Cat#: A32790 RRID: AB_2762833
Rhodamine Red™-X Donkey Anti-Guinea pig IgG (1:100)	Jackson ImmunoResearch	Cat#: 706-295-148 RRID: AB_2340468
Rhodamine Red™-X Donkey Anti-Rabbit IgG (1:100)	Jackson ImmunoResearch	Cat#: 711-295-152 RRID: AB_2340613
Rhodamine Red™-X Donkey Anti-Rat IgG (1:100)	Jackson ImmunoResearch	Cat#: 712-295-153 RRID: AB_2340676
Alexa Fluor™ Plus 555 Donkey anti-Rat IgG (1:500)	Thermo-Fisher Scientific	Cat#: A48270 RRID:AB_2896336
Alexa Fluor™ Plus 555 Donkey anti-Goat IgG (1:500)	Thermo-Fisher Scientific	Cat#: A32816 RRID:AB_2762839
Alexa Fluor® 647 Donkey Anti-Rabbit IgG (1:500)	Jackson ImmunoResearch	Cat#: 711-605-152 RRID:AB_2492288
Alexa Fluor® 647 Donkey Anti-Goat IgG (1:500)	Jackson ImmunoResearch	Cat#: 705-605-147 RRID: AB_2340437
Alexa Fluor® 647 Donkey Anti-Guinea pig IgG (1:500)	Jackson ImmunoResearch	Cat#: 706-605-148 RRID: AB_2340476
Biotin-SP Donkey Anti-Goat IgG (1:500)	Jackson ImmunoResearch	Cat#: 705-065-147 RRID: AB_2340397
Biotin-SP Donkey Anti-Guinea pig IgG (1:500)	Jackson ImmunoResearch	Cat#: 706-065-148 RRID: AB_2340451
Biotin-SP Donkey Anti-Rabbit IgG (1:500)	Jackson ImmunoResearch	Cat#: 711-065-152 RRID: AB_2340593
Avidin conjugates		
Extravidin-Peroxidase	Sigma-Aldrich	Cat#: E2886 RRID:AB_2620165

Click here to enter text.

Streptavidin-Pacific Blue	Life Technologies	Cat#: S11222
HCR probe		
Mm-Trpm8 v3.0	Molecular Instruments	
Chemicals		
Cholera toxin B subunit	Sigma-Aldrich	Cat#: C9972
DAPI	Sigma-Aldrich	Cat#: D9542
Sodium borohydride	Sigma-Aldrich	Cat#: 452882
3,3'-Diaminobenzidine	Revvity	Cat#: NEL938001EA
Hydrogen peroxide	Sigma-Aldrich	Cat#: H1009
Osmium tetroxide	Agar Scientific	Cat#: R1016
Uranyl acetate	Agar Scientific	Cat#: R1260A
Lead citrate	Agar Scientific	Cat#: R1210
Software		
Neurolucida	MBF Bioscience	https://www.mbfbioscience.com/neurolucida RRID: SCR_001775
Neurolucida Explorer	MBF Bioscience	https://www.mbfbioscience.com/neurolucida-explorer RRID: SCR_017348
pClamp	Molecular Devices	https://www.moleculardevices.com/products/axon-patch-clamp-system/acquisition-and-analysis-software/pclamp-software-suite#gref RRID: SCR_011323
Easy Electrophysiology	Easy Electrophysiology LTD	https://www.easyelectrophysiology.com
Zen Black	Carl Zeiss	https://www.zeiss.com/microscopy/int/products/microscope-software/zen.html RRID: SCR_018163
Prism	GraphPad Software	https://www.graphpad.com/scientific-software/prism/ RRID: SCR_002798
Photoshop CS6	Adobe Systems Incorporated	https://www.adobe.com/
Xara Xtreme v2.0	Xara Group Ltd	https://www.xara.com/
Inkscape	Software Freedom Conservancy	https://inkscape.org/

Experimental Model and Subject Details

All experiments were approved by the Ethical Review Process Applications Panel of the University of Glasgow, and were carried out in accordance with the UK Animals (Scientific Procedures) Act 1986 and ARRIVE guidelines. The following transgenic mouse lines were used in this study: the BAC transgenic Phox2a::Cre line, which expresses Cre recombinase under control of the Phox2a promoter[10]; the Ai9 Cre reporter line, in which a

Click here to enter text.

528 loxP-flanked STOP cassette prevents CAG promoter-driven transcription of tdTomato[61];
529 the Trpm8^{Flp} line, in which 2A-linked FlpO recombinase is fused with the last codon (and
530 replaces the stop codon) of the *Trpm8* gene[9]; the RCE:FRT line, which carries the R26R
531 CAG-boosted EGFP reporter allele with a FRT-flanked STOP cassette upstream of the
532 EGFP gene[67]; and the Calb1^{Cre} line which has an IRES2 sequence and a Cre
533 recombinase gene inserted downstream of the translational STOP codon of the calbindin 1
534 gene[68]. Further details of these lines can be found in the Key Resources table. The
535 following crosses were generated by cross-breeding these lines: Trpm8^{Flp};RCE:FRT mice,
536 which were used for anatomical analysis of Trpm8-expressing DRG cells, for
537 electrophysiological experiments, and for retrograde tracing of spinothalamic neurons;
538 Trpm8^{Flp};RCE:FRT;Ai9 mice, which were used for some electrophysiological experiments;
539 Trpm8^{Flp};RCE:FRT;Phox2a::Cre;Ai9 mice, which were used for the combined confocal and
540 electron microscopic analysis; and Calb1^{Cre};Trpm8^{Flp};RCE:FRT mice, which were used to
541 determine the proportion of retrogradely labelled Calb1-expressing cells that received
542 dense Trpm8 input.
543 Perfusion fixation was performed while mice were deeply anaesthetised with
544 pentobarbitone (20 mg i.p.). A brief rinse with Ringer's solution was followed by perfusion
545 with ~250 ml of fixative. In all cases apart from those used for combined confocal/electron
546 microscopy the fixative consisted of 4% freshly depolymerised formaldehyde in phosphate
547 buffer (PB). Spinal cords and brains were dissected and stored in the same fixative for 2
548 hours, before being transferred to 30% sucrose in PB.
549 Dorsal root ganglia for FISH were obtained from Trpm8^{Flp};RCE:FRT mice, which had
550 been killed with an overdose of pentobarbital (40 mg i.p.) and perfused with cold
551 phosphate buffered saline (PBS). The ganglia were fixed in 4% formaldehyde for 2 hours.
552 Mice of both sexes, aged 4-14 weeks and weighing between 13 and 25 g at the start of
553 any surgical procedures were used in the study.
554
555 **Fluorescent *in situ* hybridisation, immunohistochemistry and imaging**
556 FISH was performed on intact lumbar dorsal root ganglia from Trpm8^{Flp};RCE:FRT mice
557 using HCR RNA-FISH v3.0 reagents. Tissues were dehydrated in graded ethanol
558 solutions, followed by rinsing in PBS. Hybridisation and amplification were performed with
559 a probe against mouse *Trpm8* mRNA and hairpins conjugated to Alexa Fluor 546 (HCR
560 v3.0, Molecular Instruments, Inc.) according to the manufacturer's instructions. Tissues
561 were mounted using antifade mounting medium and stored at -20°C.

562 Sections of brain, spinal cord and dorsal root ganglia for immunohistochemical
563 processing were cut on either a vibrating blade microtome (Leica VT1000 or VT1200) or a
564 cryostat (Leica CM1950). Section thickness was 50 μm for brain and 60 μm for spinal cord
565 and dorsal root ganglia. Multiple-label immunofluorescence microscopy was carried out as
566 described previously[45,52,69]. Reactions were performed on free-floating sections, and the
567 sources and concentrations of antibodies are listed in the Key Resources Table. Sections
568 were incubated for 1-3 days at 4°C or room temperature in primary antibodies diluted in
569 PBS that contained 0.3M NaCl, 0.3% Triton X-100 (except for tissue processed by the
570 confocal/EM method) and 5% normal donkey serum. After rinsing they were incubated for
571 2-18 hours in appropriate species-specific secondary antibodies that were raised in
572 donkey and conjugated to Alexa Fluor Plus 405, Alexa Fluor 488, Alexa Fluor Plus 488,
573 Alexa Fluor Plus 555, Alexa Fluor 647 or Rhodamine Red, in the same diluent. Following
574 the reaction, sections were mounted with anti-fade medium and stored at -20°C.
575 Tissue sections and dorsal root ganglia that had undergone immunofluorescence
576 labelling or FISH were scanned with either a Zeiss LSM710 confocal microscope with
577 Argon multi-line, 405 nm diode, 561 nm solid state and 633 nm HeNe lasers, or with a
578 Zeiss LSM900 Airyscan confocal microscope with 405, 488, 561 and 640 nm diode lasers.
579 Confocal image stacks were obtained through a 20x dry lens (numerical aperture, NA,
580 0.8), or through 40x (NA 1.3) or 63x (NA 1.4) oil immersion lenses with the confocal
581 aperture set to 1 Airy unit or less.
582 The method for combining confocal and electron microscopy was the same as that
583 described previously[70]. Two Trpm8^{Flp};RCE:FRT;Phox2a::Cre;Ai9 mice were perfused with
584 fixative that contained 0.5% glutaraldehyde and 4% formaldehyde. Horizontal sections of
585 spinal cord were obtained from lumbar segments, and these were treated with 50%
586 ethanol for 30 mins, to enhance antibody penetration, and then with 1% sodium
587 borohydride for 30 mins to quench unbound aldehyde sites. After rinsing, they were
588 incubated for 3 days in primary antibodies against GFP (raised in rabbit) and mCherry
589 (raised in rat), and then overnight in a mixture of secondary antibodies: donkey anti-rabbit
590 conjugated to Alexa Fluor 488, donkey anti-rabbit conjugated to biotin and donkey anti-rat
591 conjugated to Rhodamine Red. Note that the anti-mCherry antibody recognises tdTomato.
592 The antibody diluent consisted of PBS that contained 0.3M NaCl and 5% normal donkey
593 serum. They were then incubated in avidin conjugated to horseradish peroxidase (HRP)
594 and mounted on slides with anti-fade medium. Sections were viewed with a confocal
595 microscope, and regions that contained tdTomato-positive cells that were densely coated

Click here to enter text.

596 with GFP-labelled axons were selected. These were scanned with the confocal
597 microscope to generate z-series through the cell bodies and dendritic trees of the neurons.
598 The sections were then removed from the slides, rinsed in PBS and then PB, processed
599 with 3,3'-diaminobenzidine (DAB) and H_2O_2 to reveal peroxidase-labelled (Trpm8-positive)
600 axons, osmicated, stained with uranyl acetate, dehydrated and flat-embedded in Durcupan
601 resin between acetate sheets[70]. Series of ultrathin sections (silver interference colour)
602 were cut with a diamond knife and collected on Formvar-coated slot grids. These were
603 further stained with lead citrate and viewed with either a Philips CM100 or Jeol JEM-
604 1400Flash electron microscope.
605
606 **Intracranial and intraspinal injections**
607 All surgical procedures involving intraspinal and/or intracranial injections were
608 performed while the mice were anaesthetised with isoflurane (1-2%), and all animals
609 received perioperative analgesia (buprenorphine 0.1 mg/kg and carprofen 10 mg/kg, s.c.).
610 For both types of injection, the mice were placed in a stereotaxic frame.
611 For intracranial injections, lidocaine (10 mg/kg, s.c.) was injected into the skin over the
612 skull, which was then incised. Burr holes were drilled to allow targeting at the following co-
613 ordinates (CVLM: 1.1-1.3 mm lateral to midline, 3.5 mm caudal to lambdoid suture, 3.3-3.7
614 mm below brain surface; LPB: 1.1 mm lateral to the midline, 0.35 mm caudal to lambdoid
615 suture or 4.5 mm caudal to bregma, 3.0 mm below brain surface, PAG: 0.4 mm lateral to
616 midline, 0.4 mm caudal to the interaural line, 3.1 mm below brain surface; VPL: 1.6-1.7
617 lateral to the midline, 0.79-1.11 caudal to bregma, 3.4 mm below brain surface). Injections
618 were made through glass micropipettes (outer tip diameter ~60 μm) attached to a Harvard
619 Pump 11 Elite (for AAV injections) or a PV 800 Pneumatic Picopump (WPI; for CTB
620 injections). Injections of AAV11.Cre^{ON}.tdTomato into LPB or PAG of
621 Calb1^{Cre};Trpm8^{Flp};RCE:FRT mice contained 2x10^9 GC in 400 nl (LPB) or 1x10^9 GC in 200
622 nl (PAG). Injections into the lateral thalamus consisted of 100 nl of 1% CTB. Micropipettes
623 were left in place for ~5 mins after the injection to limit leakage up the track. For
624 electrophysiological experiments mice were allowed to recover for between 9 and 18 days
625 (see below for further details). For anatomical experiments, survival times were 3 days for
626 CTB injections and 14-15 days for AAV injections and these were followed by perfusion
627 fixation, as described above.
628 For intraspinal injections the T12 and L1 vertebrae were exposed and clamped.
629 Injections were made through glass micropipettes (outer tip diameter ~60 μm) attached to

630 a 10 μL Hamilton syringe, on the right side of the spinal cord into either the L3 segment, or
631 the L3, L4 and L5 segments. Injections into L3 and L5 were made through the
632 intervertebral spaces on either side of the T13 vertebra, while those into L4 were made
633 through a small hole drilled in the lamina of the T13 vertebra. In initial experiments we
634 used a similar strategy to that described in previous papers[45,46], and these are referred to
635 as "central" injections. We subsequently modified the technique in order to restrict injection
636 sites to the medial part of the dorsal horn and exclude the LSN, and we refer to these as
637 "medial" injections. The mice survived between 26 and 55 days and were then deeply
638 anaesthetised and perfused with fixative as described above (for further details see Table
639 1).
640

641 **Image analysis**

642 Lamina I ALS neurons that received numerous contacts from GFP-positive (Trpm8-
643 expressing) primary afferents were identified in several parts of this study, either following
644 retrograde labelling or through expression of tdTomato (in crosses that involved
645 Phox2a::Cre and Ai9). The cells could be readily identified by the close association of
646 GFP-labelled axons with their dendrites, which received multiple contacts from GFP-
647 positive boutons. In most cases the cell bodies were also associated with numerous GFP-
648 labelled boutons, and these sometimes completely surrounded the cell body[9].
649 All quantitative image analyses were performed with Neurolucida for Confocal software
650 (MBF Bioscience, Williston, VT, USA).
651 To determine the proportion of DRG neurons that were labelled with GFP in
652 Trpm8^{Flp};RCE:FRT mice we scanned 3 or 4 sections immunostained to reveal GFP and
653 NeuN, and counterstained with DAPI from the L4 dorsal root ganglia from each of 3 mice
654 (1 male, 2 female) with a confocal microscope. Z-stacks that included the complete cross-
655 sectional area of the ganglion were analysed using a modified disector method[71].
656 Reference and look-up sections were set 10 μm apart, and all intervening sections were
657 examined to reveal any neurons that might have been located between these two levels.
658 Initially we viewed the NeuN and DAPI channels, and in this way, we identified all neurons
659 (between 904 and 1383 per mouse) for which the top surface of the nucleus was located
660 between reference and look-up section. We then revealed the channel for GFP and
661 counted any of the sampled neurons that were GFP-immunoreactive.
662 For the comparison of *Trpm8* mRNA and GFP dorsal root ganglia from 3
663 Trpm8^{Flp};RCE:FRT mice (1 male, 2 female) that had been reacted as described above

Click here to enter text.

were scanned with a confocal microscope to generate z-series through the entire volume of the ganglion. Initially, both fluorescent channels (GFP and Alexa Fluor 546) were combined such that any cell with either GFP or *Trpm8* mRNA was visible. For all of these cells (between 155-209 per mouse), the cell size was determined by drawing an outline of the cell at its maximum point and converting cross-sectional area to diameter by assuming a circular shape. The two fluorescent channels were then separated, and for each cell the presence of GFP and/or *Trpm8* mRNA was determined.

Because we found a relatively limited range of sizes for GFP/*Trpm8*-positive cells (see Figure 1C) we did not use a stereological method for analysing co-localisation with other neurochemical markers. We scanned sections of dorsal root ganglia immunoreacted to reveal GFP together with: (1) VGLUT3, (2) Trpv1, (3) CGRP and substance P, or (4) somatostatin. In each case tissue from 3 mice (either 2 male and 1 female, or 1 male and 2 female) was used, and z-stacks covering the entire cross-sectional area of the ganglion were analysed. Initially the GFP channel was viewed and the locations of all labelled cells were marked (between 126 and 350 per mouse for each reaction). The other channel(s) was/were then examined and the presence or absence of the other marker(s) was noted.

To determine the proportion of retrogradely labelled lamina I neurons that had dense input from Trpm8-expressing afferents in the Calb1^{Cre};Trpm8^{Flp};RCE:FRT mice injected with AAV11.Cre^{ON}.tdTomato into either LPB (4 mice, 2 male and 2 female) or PAG (3 mice, 1 male, 2 female), we examined horizontal sections cut through the L2, L3 and L4 segments. These had been immunostained to reveal GFP and tdTomato, and were scanned with a confocal microscope. The resulting z-stacks were viewed with Neurolucida software, initially with only the tdTomato channel visible, and the locations of retrogradely labelled lamina I neurons were recorded (between 32 and 81 cells per segment in each animal for the experiments involving LPB injections). For the experiments involving PAG injections, numbers of retrogradely labelled neurons were much lower, and results from the 3 segments were pooled for each animal (between 26 and 99 cells per mouse). The GFP channel was then viewed, and cells that received dense Trpm8 input were identified. The L5 segments of the 4 Calb1^{Cre};Trpm8^{Flp};RCE:FRT mice that had received injections into LPB mice were cut transversely and the locations of tdTomato-labelled cell bodies on between 8 and 10 individual sections were identified. These were then morphed onto a standard outline of the L5 segment in Inkscape, resulting in single scalable vector graphics files for each mouse.

697 To test whether cold-selective cells were included among those projecting to the lateral
698 thalamus, we examined horizontal sections from the L4 and C7 segments of 3
699 Trpm8^{Flp};RCE:FRT mice (2 male, 1 female) that had received CTB injections into the
700 lateral thalamus. Sections were immunoreacted to reveal CTB and GFP and scanned with
701 a confocal microscope. We then searched for CTB-labelled cells that were associated with
702 numerous GFP-positive axons.
703 For anterograde tracing following intraspinal injections of AAV1.Cre^{ON}.tdTomato in
704 Calb1^{Cre} mice, sections were first viewed with a fluorescence microscope (Zeiss Axioscope
705 5) and selected sections were scanned with a confocal microscope. Identification of brain
706 regions that contained tdTomato-labelled axons was generally based on the atlas of
707 Franklin and Paxinos[55], apart from the LPB. For this, we used the same terminology as in
708 our previous paper[46], and identified the PBrel nucleus based on the findings of Geerling et
709 al[42].
710
711 **Semi-intact somatosensory preparation**
712 The semi-intact somatosensory preparation was made as described previously[27,28] with
713 minor modifications. Mice were anaesthetised with isoflurane, followed by a lethal dose of
714 pentobarbital, and then quickly perfused with oxygenated sucrose-based artificial
715 cerebrospinal fluid (ACSF; in mM; 3.0 KCl, 1.2 NaH_2PO_4, 0.5 $CaCl_2$, 7.0 $MgCl_2$, 26.0
716 $NaHCO_3$, 15.0 glucose, 251.6 sucrose, 1.0 Na ascorbate, and 1.0 Na pyruvate). The back
717 skin was incised, and the spinal cord was exposed by dorsal laminectomy. The right
718 hindlimb and the right side of the trunk with the spinal cord were excised and transferred to
719 the dissection/recording chamber, and tissues were submerged in the oxygenated
720 sucrose-based ACSF. The right hind paw skin, saphenous nerve, and femoral cutaneous
721 nerve were carefully isolated from the surrounding tissues. Only the L2 and L3 ganglia on
722 the right side were left attached to the spine. All dorsal roots except L2 and L3, dural and
723 pial membranes were carefully removed. The spinal cord was pinned onto a Sylgard
724 chamber with the right dorsal horn facing upward. The tissued was perfused with
725 oxygenated normal ACSF (in mM; 125.8 NaCl, 3.0 KCl, 1.2 NaH_2PO_4, 2.4 $CaCl_2$, 1.3
726 $MgCl_2$, 26.0 $NaHCO_3$, and 15.0 glucose) at 25˚C. Recordings were performed for up to 4
727 hours after dissection.
728

729 **Patch-clamp recording from lamina I projection neurons**

730 To test whether cells with dense Trpm8 input were cold-selective, we made patch-clamp
731 recordings in 4 Trpm8^{Flp};RCE:FRT mice (1 male, 3 female) that had received injections of
732 AAV9.mCherry into the LPB or CVLM, and one male Trpm8^{Flp};RCE:FRT;Ai9 mouse
733 injected in the CVLM with AAV9.EGFP_Cre. For the investigation of Calb1-Cre-positive
734 lamina I neurons, recordings were made in 4 female Calb1^{Cre} mice that had received
735 injections of AAV11.Cre^{ON}.tdTomato into the CVLM.

736 Neurons were visualised using a fixed stage upright microscope (SliceScope;
737 Scientifica, Uckfield, UK) equipped with a 40x water immersion objective and a CMOS
738 Camera (Prime BSI Express, Teledyne Vision Solutions, Ontario, Canada). A narrow-
739 beam infrared LED (Opto SFH 4550; Osram, Munich, Germany, emission peak, 860 nm)
740 was positioned outside the solution meniscus. Fluorescent cells and axons were visualised
741 using LED illumination (pE-300 ultra, CoolLED, Andover, UK). Whole-cell patch clamp
742 recordings were made with a pipette constructed from thin-walled single-filamented
743 borosilicate glass using a microelectrode puller (P-1000, Sutter Instrument, CA, USA).
744 Pipette resistances ranged from 6 to 10 MΩ. Electrodes were filled with an intracellular
745 solution (in mM; 130.0 K gluconate, 10.0 KCl, 2.0 $MgCl_2$, 10.0 HEPES, 0.5 EGTA, 2.0
746 ATP-Na, 0.5 GTP-Na, and 0.2% Neurobiotin, pH adjusted to 7.3 with 1.0 M KOH). Data
747 were recorded and acquired with an amplifier (Axopatch 200B; Molecular Devices,
748 Wokingham, UK). The data were low-pass filtered at 2 kHz and digitised at 10 kHz with an
749 A/D converter (Digidata 1550B; Molecular Devices, Wokingham, UK) and stored using a
750 data acquisition program (Clampex 11; Molecular Devices, Wokingham, UK). Recordings
751 were initially made in voltage clamp mode (VH = -70mV) to reveal spontaneous EPSCs.
752 To find the receptive field of the recorded neurons, mechanical, hot, and cold stimuli were
753 gently applied to the skin. Mechanical stimulation was applied using von Frey filaments (4-
754 g or 10-g), and in some cases the skin was brushed with a paintbrush. Hot and cold
755 stimulation were administered by applying a small amount of 15˚C saline or 50˚C saline to
756 the skin using an eye dropper. The temperature at the skin surface was 20˚C and 38˚C,
757 respectively. Once the receptive field was identified, each stimulus was reapplied directly
758 to the receptive field for 1 second. The evoked EPSCs were recorded in voltage clamp
759 mode (VH = -70mV), and the evoked action potentials were recorded in current clamp
760 mode (IH = 0 pA) or both. The events were detected with Easy Electrophysiology software
761 (Easy Electrophysiology, London, UK).

762

Click here to enter text.

763 **Quantification and statistical analysis**

764 Data are reported as mean ± SD, unless stated otherwise. Statistical analyses were
765 performed using Prism software (v10, GraphPad Software, CA, USA) or SciPy library
766 (https://docs.scipy.org/doc/) in Python. The statistical tests used for each experiment,
767 including tests for multiple comparisons, are given in the appropriate figure legends. A p
768 value of <0.05 was considered significant, and significance markers are denoted within
769 figures as follows: *p < 0.05, **p < 0.01, ***p < 0.001.

770

771 **Data and materials availability**

772 Upon acceptance of this manuscript, all data will be made accessible from the Enlighten:
773 Research Data open repository hosted at the University of Glasgow. This study did not
774 generate any new materials, reagents or code.

775

776

777 **ACKNOWLEDGMENTS**

778 This research was funded in whole, or in part, by the Wellcome Trust (Grant number
779 219433/Z/19/Z) and the Medical Research Council (Grant number MR/V033638/1). For the
780 purpose of Open Access, the authors have applied a CC BY public copyright licence to
781 any Author Accepted Manuscript version arising from this submission. We are grateful to
782 Robert Kerr, Iain Plenderleith and Erin Dunn for expert technical assistance, and to Mark
783 Hoon and Artur Kania for the gifts of Trpm8^{Flp} and Phox2a::Cre mice.

784

785 **AUTHOR CONTRIBUTIONS**

786 A.N.R., W.M., A.C.D., E.P, A.M.B., A.J.T and J.H. conceived the project and designed
787 experiments. A.J.T. and J.H. obtained funding. A.N.R., W.M., A.C.D., E.P., A.M., M.Y.,
788 A.H.C., D.S., A.M.B. and J.H. performed experiments. A.N.R., W.M., A.M., A.J.T. and J.H.
789 analysed data. M.W. provided reagents. A.N.R., W.M., A.M.B., A.J.T. and J.H. wrote the
790 paper. All of the authors provided feedback and contributed to editing of the manuscript.

791

792 **COMPETING INTERESTS**

793 The authors declare no competing interests.

794

795 **REFERENCES**

796 1. Javed, S., Viswanathan, A., and Abdi, S. (2020). Cordotomy for intractable cancer pain: a narrative
797 review. Pain Physician *23*, 283-292.
798 2. Lahuerta, J., Bowsher, D., Campbell, J., and Lipton, S. (1990). Clinical and instrumental evaluation of
799 sensory function before and after percutaneous anterolateral cordotomy at cervical level in man.
800 Pain *42*, 23-30. 10.1016/0304-3959(90)91087-Y.
801 3. Chung, K., Kevetter, G.A., Willis, W.D., and Coggeshall, R.E. (1984). An estimate of the ratio of
802 propriospinal to long tract neurons in the sacral spinal cord of the rat. Neuroscience letters *44*, 173-
803 177. 10.1016/0304-3940(84)90077-6.
804 4. Abraira, V.E., and Ginty, D.D. (2013). The sensory neurons of touch. Neuron *79*, 618-639.
805 10.1016/j.neuron.2013.07.051.
806 5. Ma, Q. (2022). A functional subdivision within the somatosensory system and its implications for
807 pain research. Neuron *110*, 749-769. 10.1016/j.neuron.2021.12.015.
808 6. Todd, A.J. (2010). Neuronal circuitry for pain processing in the dorsal horn. Nature reviews.
809 Neuroscience *11*, 823-836. nrn2947 [pii] 10.1038/nrn2947.
810 7. Wang, L.H., Ding, W.Q., and Sun, Y.G. (2022). Spinal ascending pathways for somatosensory
811 information processing. Trends Neurosci *45*, 594-607. 10.1016/j.tins.2022.05.005.
812 8. Wercberger, R., and Basbaum, A.I. (2019). Spinal cord projection neurons: a superficial, and also
813 deep, analysis. Curr Opin Physiol *11*, 109-115. 10.1016/j.cophys.2019.10.002.
814 9. Bell, A.M., Utting, C., Dickie, A.C., Kucharczyk, M.W., Quillet, R., Gutierrez-Mecinas, M., Razlan,
815 A.N.B., Cooper, A.H., Lan, Y., Hachisuka, J., et al. (2024). Deep sequencing of Phox2a nuclei reveals
816 five classes of anterolateral system neurons. Proceedings of the National Academy of Sciences of
817 the United States of America *121*, e2314213121. 10.1073/pnas.2314213121.
818 10. Roome, R.B., Bourojeni, F.B., Mona, B., Rastegar-Pouyani, S., Blain, R., Dumouchel, A., Salesse, C.,
819 Thompson, W.S., Brookbank, M., Gitton, Y., et al. (2020). Phox2a defines a developmental origin of
820 the anterolateral system in mice and humans. Cell reports *33*, 108425.
821 10.1016/j.celrep.2020.108425.
822 11. Peier, A.M., Moqrich, A., Hergarden, A.C., Reeve, A.J., Andersson, D.A., Story, G.M., Earley, T.J.,
823 Dragoni, I., McIntyre, P., Bevan, S., and Patapoutian, A. (2002). A TRP channel that senses cold
824 stimuli and menthol. Cell *108*, 705-715. 10.1016/s0092-8674(02)00652-9.
825 12. McKemy, D.D., Neuhausser, W.M., and Julius, D. (2002). Identification of a cold receptor reveals a
826 general role for TRP channels in thermosensation. Nature *416*, 52-58. 10.1038/nature719.
827 13. Lewis, C.M., and Griffith, T.N. (2022). The mechanisms of cold encoding. Current opinion in
828 neurobiology *75*, 102571. 10.1016/j.conb.2022.102571.
829 14. Knowlton, W.M., Palkar, R., Lippoldt, E.K., McCoy, D.D., Baluch, F., Chen, J., and McKemy, D.D.
830 (2013). A sensory-labeled line for cold: TRPM8-expressing sensory neurons define the cellular basis
831 for cold, cold pain, and cooling-mediated analgesia. The Journal of neuroscience : the official
832 journal of the Society for Neuroscience *33*, 2837-2848. 10.1523/JNEUROSCI.1943-12.2013.
833 15. Pogorzala, L.A., Mishra, S.K., and Hoon, M.A. (2013). The cellular code for mammalian
834 thermosensation. The Journal of neuroscience : the official journal of the Society for Neuroscience
835 *33*, 5533-5541. 10.1523/JNEUROSCI.5788-12.2013.
836 16. Takashima, Y., Daniels, R.L., Knowlton, W., Teng, J., Liman, E.R., and McKemy, D.D. (2007). Diversity
837 in the neural circuitry of cold sensing revealed by genetic axonal labeling of transient receptor
838 potential melastatin 8 neurons. The Journal of neuroscience : the official journal of the Society for
839 Neuroscience *27*, 14147-14157. 10.1523/JNEUROSCI.4578-07.2007.
840 17. Kim, Y.S., Park, J.H., Choi, S.J., Bae, J.Y., Ahn, D.K., McKemy, D.D., and Bae, Y.C. (2014). Central
841 connectivity of transient receptor potential melastatin 8-expressing axons in the brain stem and
842 spinal dorsal horn. PloS one *9*, e94080. 10.1371/journal.pone.0094080.

18. Dhaka, A., Earley, T.J., Watson, J., and Patapoutian, A. (2008). Visualizing cold spots: TRPM8-expressing sensory neurons and their projections. The Journal of neuroscience : the official journal of the Society for Neuroscience *28*, 566-575. 28/3/566 [pii] 10.1523/JNEUROSCI.3976-07.2008.
19. Craig, A.D., and Kniffki, K.D. (1985). Spinothalamic lumbosacral lamina I cells responsive to skin and muscle stimulation in the cat. The Journal of physiology *365*, 197-221. 10.1113/jphysiol.1985.sp015767.
20. Craig, A.D., Krout, K., and Andrew, D. (2001). Quantitative response characteristics of thermoreceptive and nociceptive lamina I spinothalamic neurons in the cat. Journal of neurophysiology *86*, 1459-1480. 10.1152/jn.2001.86.3.1459.
21. Craig, A.D., and Dostrovsky, J.O. (2001). Differential projections of thermoreceptive and nociceptive lamina I trigeminothalamic and spinothalamic neurons in the cat. Journal of neurophysiology *86*, 856-870. 10.1152/jn.2001.86.2.856.
22. Craig, A.D., and Hunsley, S.J. (1991). Morphine enhances the activity of thermoreceptive cold-specific lamina I spinothalamic neurons in the cat. Brain research *558*, 93-97. 10.1016/0006-8993(91)90719-c.
23. Dostrovsky, J.O., and Craig, A.D. (1996). Cooling-specific spinothalamic neurons in the monkey. Journal of neurophysiology *76*, 3656-3665. 10.1152/jn.1996.76.6.3656.
24. Zhang, X., Davidson, S., and Giesler, G.J., Jr. (2006). Thermally identified subgroups of marginal zone neurons project to distinct regions of the ventral posterior lateral nucleus in rats. The Journal of neuroscience : the official journal of the Society for Neuroscience *26*, 5215-5223. 10.1523/JNEUROSCI.0701-06.2006.
25. Allard, J. (2019). Physiological properties of the lamina I spinoparabrachial neurons in the mouse. The Journal of physiology *597*, 2097-2113. 10.1113/JP277447.
26. Andrew, D. (2009). Sensitization of lamina I spinoparabrachial neurons parallels heat hyperalgesia in the chronic constriction injury model of neuropathic pain. The Journal of physiology *587*, 2005-2017.
27. Hachisuka, J., Baumbauer, K.M., Omori, Y., Snyder, L.M., Koerber, H.R., and Ross, S.E. (2016). Semi-intact ex vivo approach to investigate spinal somatosensory circuits. Elife *5*, e22866. 10.7554/eLife.22866.
28. Hachisuka, J., Koerber, H.R., and Ross, S.E. (2020). Selective-cold output through a distinct subset of lamina I spinoparabrachial neurons. Pain *161*, 185-194. 10.1097/j.pain.0000000000001710.
29. Chisholm, K.I., Lo Re, L., Polgar, E., Gutierrez-Mecinas, M., Todd, A.J., and McMahon, S.B. (2021). The encoding of cutaneous stimuli by lamina I projection neurons. Pain *162*, 2405-2417. 10.1097/j.pain.0000000000002226.
30. Lee, H., Hor, C.C., Horwitz, L.R., Xiong, A., Su, X.Y., Soden, D.R., Yang, S., Cai, W., Zhang, W., Li, C., et al. (2025). A dedicated skin-to-brain circuit for cool sensation in mice. Nature communications *16*, 6731. 10.1038/s41467-025-61562-y.
31. Qi, L., Iskols, M., Shi, D., Reddy, P., Walker, C., Lezgiyeva, K., Voisin, T., Pawlak, M., Kuchroo, V.K., Chiu, I.M., et al. (2024). A mouse DRG genetic toolkit reveals morphological and physiological diversity of somatosensory neuron subtypes. Cell *187*, 1508-1526 e1516. 10.1016/j.cell.2024.02.006.
32. Sharma, N., Flaherty, K., Lezgiyeva, K., Wagner, D.E., Klein, A.M., and Ginty, D.D. (2020). The emergence of transcriptional identity in somatosensory neurons. Nature *577*, 392-398. 10.1038/s41586-019-1900-1.
33. Zeisel, A., Hochgerner, H., Lonnerberg, P., Johnsson, A., Memic, F., van der Zwan, J., Haring, M., Braun, E., Borm, L.E., La Manno, G., et al. (2018). Molecular Architecture of the Mouse Nervous System. Cell *174*, 999-1014 e1022. 10.1016/j.cell.2018.06.021.
34. Li, J., Kritzer, E., Craig, P.E., and Baccei, M.L. (2015). Aberrant synaptic integration in adult lamina I projection neurons following neonatal tissue damage. The Journal of neuroscience : the official journal of the Society for Neuroscience *35*, 2438-2451. 10.1523/JNEUROSCI.3585-14.2015.

35. Seal, R.P., Wang, X., Guan, Y., Raja, S.N., Woodbury, C.J., Basbaum, A.I., and Edwards, R.H. (2009). Injury-induced mechanical hypersensitivity requires C-low threshold mechanoreceptors. Nature *462*, 651-655.
36. Dickie, A.C., Bell, A.M., Iwagaki, N., Polgar, E., Gutierrez-Mecinas, M., Kelly, R., Lyon, H., Turnbull, K., West, S.J., Etlin, A., et al. (2019). Morphological and functional properties distinguish the substance P and gastrin-releasing peptide subsets of excitatory interneuron in the spinal cord dorsal horn. Pain *160*, 442-462. 10.1097/j.pain.0000000000001406.
37. Gutierrez-Mecinas, M., Kuehn, E.D., Abraira, V.E., Polgár, E., Watanabe, M., and Todd, A.J. (2016). Immunostaining for Homer reveals the majority of excitatory synapses in laminae I-III of the mouse spinal dorsal horn. Neuroscience *329*, 171-181. 10.1016/j.neuroscience.2016.05.009.
38. Todd, A.J. (1997). A method for combining confocal and electron microscopic examination of sections processed for double- or triple-labelling immunocytochemistry. Journal of neuroscience methods *73*, 149-157. S0165-0270(97)02222-X [pii].
39. Menetrey, D., De Pommery, J., Thomasset, M., and Baimbridge, K.G. (1992). Calbindin-D28K (CaBP28k)-like Immunoreactivity in Ascending Projections. The European journal of neuroscience *4*, 70-76. 10.1111/j.1460-9568.1992.tb00110.x.
40. Alsulaiman, W.A.A., Quillet, R., Bell, A.M., Dickie, A.C., Polgar, E., Boyle, K.A., Watanabe, M., Roome, R.B., Kania, A., Todd, A.J., and Gutierrez-Mecinas, M. (2021). Characterisation of lamina I anterolateral system neurons that express Cre in a Phox2a-Cre mouse line. Scientific reports *11*, 17912. 10.1038/s41598-021-97105-w.
41. Cano, G., Passerin, A.M., Schiltz, J.C., Card, J.P., Morrison, S.F., and Sved, A.F. (2003). Anatomical substrates for the central control of sympathetic outflow to interscapular adipose tissue during cold exposure. The Journal of comparative neurology *460*, 303-326. 10.1002/cne.10643.
42. Geerling, J.C., Kim, M., Mahoney, C.E., Abbott, S.B., Agostinelli, L.J., Garfield, A.S., Krashes, M.J., Lowell, B.B., and Scammell, T.E. (2016). Genetic identity of thermosensory relay neurons in the lateral parabrachial nucleus. Am J Physiol Regul Integr Comp Physiol *310*, R41-54. 10.1152/ajpregu.00094.2015.
43. Yang, W.Z., Xie, H., Du, X., Zhou, Q., Xiao, Y., Zhao, Z., Jia, X., Xu, J., Zhang, W., Cai, S., et al. (2023). A parabrachial-hypothalamic parallel circuit governs cold defense in mice. Nature communications *14*, 4924. 10.1038/s41467-023-40504-6.
44. Yoshida, K., Konishi, M., Nagashima, K., Saper, C.B., and Kanosue, K. (2005). Fos activation in hypothalamic neurons during cold or warm exposure: projections to periaqueductal gray matter. Neuroscience *133*, 1039-1046. 10.1016/j.neuroscience.2005.03.044.
45. Ma, W., Polgar, E., Dickie, A.C., Hajer, M.A., Quillet, R., Gutierrez-Mecinas, M., Yadav, M., Hachisuka, J., Todd, A.J., and Bell, A.M. (2025). Anatomical characterisation of somatostatin-expressing neurons belonging to the anterolateral system. Scientific reports *15*, 9549. 10.1038/s41598-025-93816-6.
46. Ma, W., Dickie, A., Polgar, E., Yadav, M., Quillet, R., Gutierrez-Mecinas, M., Bell, A.M., and Todd, A. (2025). Expression of Tacr1 and Gpr83 by spinal projection neurons. Molecular pain, 17448069251342409. 10.1177/17448069251342409.
47. Bernard, J.F., Dallel, R., Raboisson, P., Villanueva, L., and Le Bars, D. (1995). Organization of the efferent projections from the spinal cervical enlargement to the parabrachial area and periaqueductal gray: a PHA-L study in the rat. The Journal of comparative neurology *353*, 480-505. 10.1002/cne.903530403.
48. Feil, K., and Herbert, H. (1995). Topographic organization of spinal and trigeminal somatosensory pathways to the rat parabrachial and Kolliker-Fuse nuclei. The Journal of comparative neurology *353*, 506-528. 10.1002/cne.903530404.
49. Gauriau, C., and Bernard, J.F. (2004). A comparative reappraisal of projections from the superficial laminae of the dorsal horn in the rat: the forebrain. The Journal of comparative neurology *468*, 24-56. 10.1002/cne.10873.
50. Gutierrez-Mecinas, M., Polgar, E., Bell, A.M., Herau, M., and Todd, A.J. (2018). Substance P-expressing excitatory interneurons in the mouse superficial dorsal horn provide a propriospinal

input to the lateral spinal nucleus. Brain structure & function *223*, 2377-2392. 10.1007/s00429-018-1629-x.

51. Gutierrez-Mecinas, M., Bell, A., Polgar, E., Watanabe, M., and Todd, A.J. (2019). Expression of neuropeptide FF defines a population of excitatory interneurons in the superficial dorsal horn of the mouse spinal cord that respond to noxious and pruritic stimuli. Neuroscience *416*, 281-293. 10.1016/j.neuroscience.2019.08.013.

52. Polgár, E., Dickie, A.C., Gutierrez-Mecinas, M., Bell, A.M., Boyle, K.A., Quillet, R., Ab Rashid, E., Clark, R.A., German, M.T., Watanabe, M., et al. (2023). Grpr expression defines a population of superficial dorsal horn vertical cells that have a role in both itch and pain. Pain *164*, 149-170. 10.1097/j.pain.0000000000002677.

53. Choi, S., Hachisuka, J., Brett, M.A., Magee, A.R., Omori, Y., Iqbal, N.U., Zhang, D., DeLisle, M.M., Wolfson, R.L., Bai, L., et al. (2020). Parallel ascending spinal pathways for affective touch and pain. Nature *587*, 258-263. 10.1038/s41586-020-2860-1.

54. Al-Khater, K.M., Kerr, R., and Todd, A.J. (2008). A quantitative study of spinothalamic neurons in laminae I, III, and IV in lumbar and cervical segments of the rat spinal cord. The Journal of comparative neurology *511*, 1-18.

55. Franklin, K.B.J., and Paxinos, G. (2007). The Mouse Brain in Stereotaxic Coordinates. Third Edition (Elsevier).

56. Ding, Y.Q., Takada, M., Shigemoto, R., and Mizumo, N. (1995). Spinoparabrachial tract neurons showing substance P receptor-like immunoreactivity in the lumbar spinal cord of the rat. Brain research *674*, 336-340. 000689939500022I [pii].

57. Marshall, G.E., Shehab, S.A., Spike, R.C., and Todd, A.J. (1996). Neurokinin-1 receptors on lumbar spinothalamic neurons in the rat. Neuroscience *72*, 255-263. 0306452295005587 [pii].

58. Al-Khater, K.M., and Todd, A.J. (2009). Collateral projections of neurons in laminae I, III, and IV of rat spinal cord to thalamus, periaqueductal gray matter, and lateral parabrachial area. The Journal of comparative neurology *515*, 629-646.

59. McKemy, D.D. (2013). The molecular and cellular basis of cold sensation. ACS Chem Neurosci *4*, 238-247. 10.1021/cn300193h.

60. Ren, X., Liu, S., Virlogeux, A., Kang, S.J., Brusch, J., Liu, Y., Dymecki, S.M., Han, S., Goulding, M., and Acton, D. (2023). Identification of an essential spinoparabrachial pathway for mechanical itch. Neuron *111*, 1812-1829 e1816. 10.1016/j.neuron.2023.03.013.

61. Madisen, L., Zwingman, T.A., Sunkin, S.M., Oh, S.W., Zariwala, H.A., Gu, H., Ng, L.L., Palmiter, R.D., Hawrylycz, M.J., Jones, A.R., et al. (2010). A robust and high-throughput Cre reporting and characterization system for the whole mouse brain. Nature neuroscience *13*, 133-140. nn.2467 [pii] 10.1038/nn.2467.

62. Morrison, S.F. (2018). Efferent neural pathways for the control of brown adipose tissue thermogenesis and shivering. Handb Clin Neurol *156*, 281-303. 10.1016/B978-0-444-63912-7.00017-5.

63. Li, J., Serafin, E.K., and Baccei, M.L. (2023). Intrinsic and synaptic properties of adult mouse spinoperiaqueductal gray neurons and the influence of neonatal tissue damage. Pain *164*, 905-917. 10.1097/j.pain.0000000000002787.

64. Spike, R.C., Puskar, Z., Andrew, D., and Todd, A.J. (2003). A quantitative and morphological study of projection neurons in lamina I of the rat lumbar spinal cord. The European journal of neuroscience *18*, 2433-2448.

65. Chen, X.M., Nishi, M., Taniguchi, A., Nagashima, K., Shibata, M., and Kanosue, K. (2002). The caudal periaqueductal gray participates in the activation of brown adipose tissue in rats. Neuroscience letters *331*, 17-20. 10.1016/s0304-3940(02)00757-7.

66. Leva, T.M., and Whitmire, C.J. (2023). Thermosensory thalamus: parallel processing across model organisms. Front Neurosci *17*, 1210949. 10.3389/fnins.2023.1210949.

67. Sousa, V.H., Miyoshi, G., Hjerling-Leffler, J., Karayannis, T., and Fishell, G. (2009). Characterization of Nkx6-2-derived neocortical interneuron lineages. Cerebral cortex *19 Suppl 1*, i1-10. 10.1093/cercor/bhp038.

997 68. Daigle, T.L., Madisen, L., Hage, T.A., Valley, M.T., Knoblich, U., Larsen, R.S., Takeno, M.M., Huang, L.,
998 Gu, H., Larsen, R., et al. (2018). A suite of transgenic driver and reporter mouse lines with enhanced
999 brain-cell-type targeting and functionality. Cell *174*, 465-480 e422. 10.1016/j.cell.2018.06.035.
1000 69. Quillet, R., Gutierrez-Mecinas, M., Polgar, E., Dickie, A.C., Boyle, K.A., Watanabe, M., and Todd, A.J.
1001 (2023). Synaptic circuits involving gastrin-releasing peptide receptor-expressing neurons in the
1002 dorsal horn of the mouse spinal cord. Front Mol Neurosci *16*, 1294994.
1003 10.3389/fnmol.2023.1294994.
1004 70. Bell, A.M., Gutierrez-Mecinas, M., Stevenson, A., Casas-Benito, A., Wildner, H., West, S.J.,
1005 Watanabe, M., and Todd, A.J. (2020). Expression of green fluorescent protein defines a specific
1006 population of lamina II excitatory interneurons in the GRP::eGFP mouse. Scientific reports *10*,
1007 13176. 10.1038/s41598-020-69711-7.
1008 71. Polgár, E., Gray, S., Riddell, J.S., and Todd, A.J. (2004). Lack of evidence for significant neuronal loss
1009 in laminae I-III of the spinal dorsal horn of the rat in the chronic constriction injury model. Pain *111*,
1010 144-150. 10.1016/j.pain.2004.06.011 S0304395904002994 [pii].

1011

1012

1013 **MAIN FIGURES**

1014 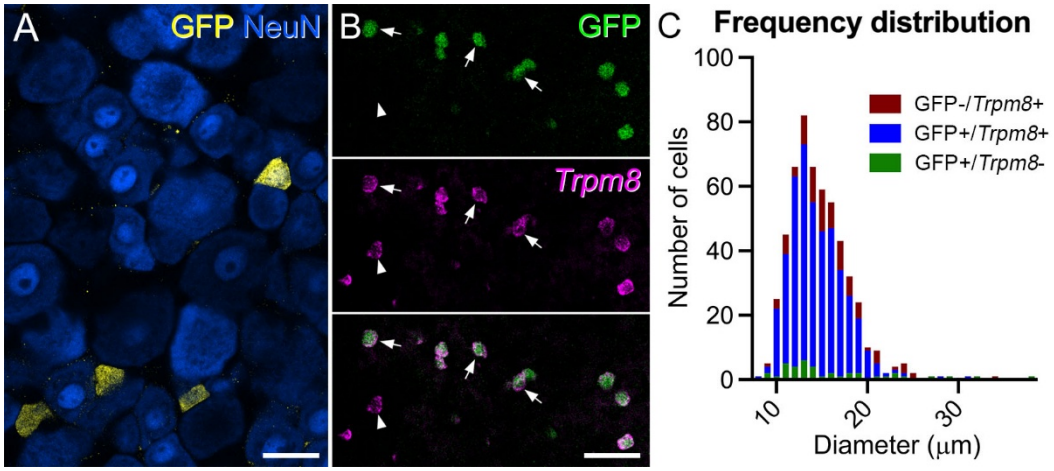

1015 **Figure 1. The Trpm8^{Flp} mouse line captures Trpm8-expressing primary afferent**
1016 **neurons.** (**A**) Immunohistochemical staining for GFP (yellow) and NeuN (blue) in a dorsal
1017 root ganglion from a Trpm8^{Flp};RCE:FRT mouse. GFP is present in some of the small
1018 neurons. (**B**) Fluorescence *in situ* hybridisation with a probe for *Trpm8* mRNA (magenta)
1019 superimposed on GFP native fluorescence (green). The great majority of GFP cells
1020 contain *Trpm8* message, and *vice versa*. Some of the double-labelled cells are indicated
1021 with arrows, while the arrowhead points to a *Trpm8*-positive cell that lacks GFP. (**C**)
1022 Frequency distribution of soma diameter for cells that were GFP-/*Trpm8*+ (red bars),
1023 GFP+/*Trpm8*+ (blue bars) or GFP+/*Trpm8*- (green bars). Scale bars: (**A**) = 25 μm, (**B**) = 50
1024 μm.

1025

Click here to enter text.

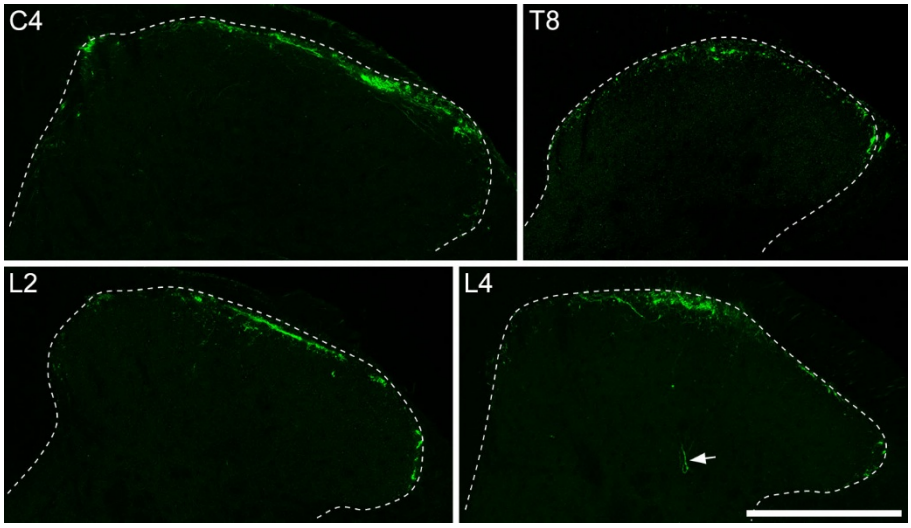

Figure 2. Distribution of Trpm8 afferents in the spinal dorsal horn.
Immunohistochemical staining for GFP at different segmental levels through the spinal cord in Trpm8^{Flp};RCE:FRT mice. GFP-labelled axons are largely restricted to lamina I, although occasional fibres penetrate into deeper parts of the dorsal horn (arrow). Within lamina I the distribution of GFP axons is patchy, and does not occupy the entire mediolateral extent. Scale bar = 200 μm.

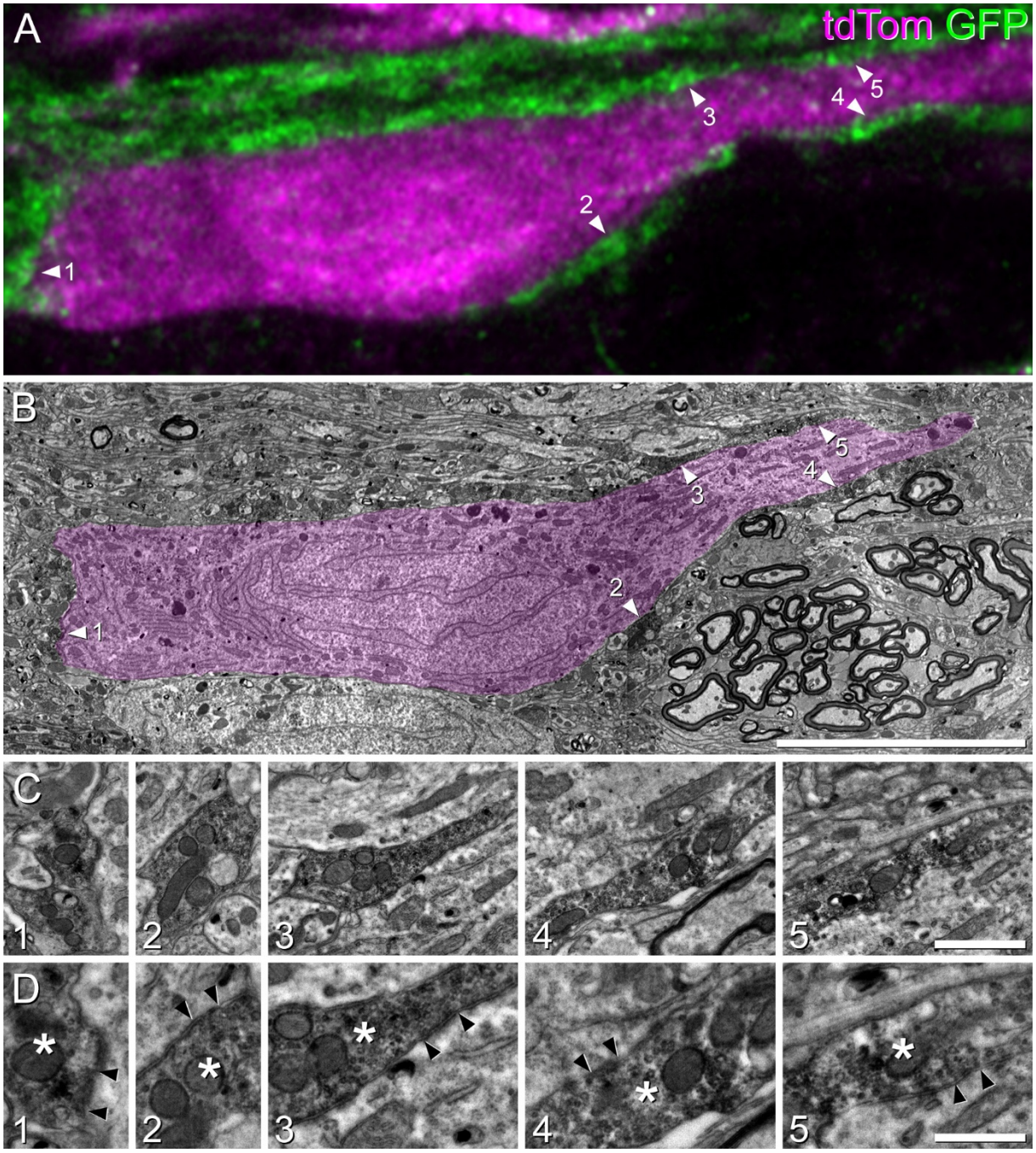

Figure 3. Combined confocal and electron microscopic examination of a lamina I projection neuron with numerous contacts from Trpm8-expressing afferents. (**A**) A confocal image (single optical section) from a horizontal section through lamina I, showing the cell body and part of a proximal dendrite of one of the tdTomato-expressing neurons that were analysed. The tissue was obtained from a Phox2a::Cre;Ai9;Trpm8^{Flp};RCE:FRT mouse. TdTomato expressed by the projection neuron is shown in magenta and GFP immunoreactivity in Trpm8 afferents in green. Several Trpm8 boutons contact the cell, and five of these are indicated with arrowheads. (**B**) A low magnification electron micrograph through the cell at approximately the same z-level as that shown in **A**. Although the cell

Click here to enter text.

1045 does not contain an electron dense label, it can be recognised by its shape, and because it
1046 is surrounded by GFP-expressing axonal profiles that were labelled with an
1047 immunoperoxidase method. The locations of those corresponding to the boutons shown in
1048 **A** are again marked with arrowheads. The cell has been pseudocoloured magenta to show
1049 its location. (**C**,**D**) Progressively higher magnification EM images showing the five GFP-
1050 labelled boutons marked with arrowheads in **A** and **B**. In **D** the boutons are marked with
1051 asterisks and the locations of membrane darkening and vesicle clusters that presumably
1052 correspond to synapses on the cell body and dendrite of the projection neuron are
1053 indicated with arrowheads. Scale bars: (**A**,**B**) = 10 μm, (**C**) = 1 μm (**D**) = 500 nm.
1054

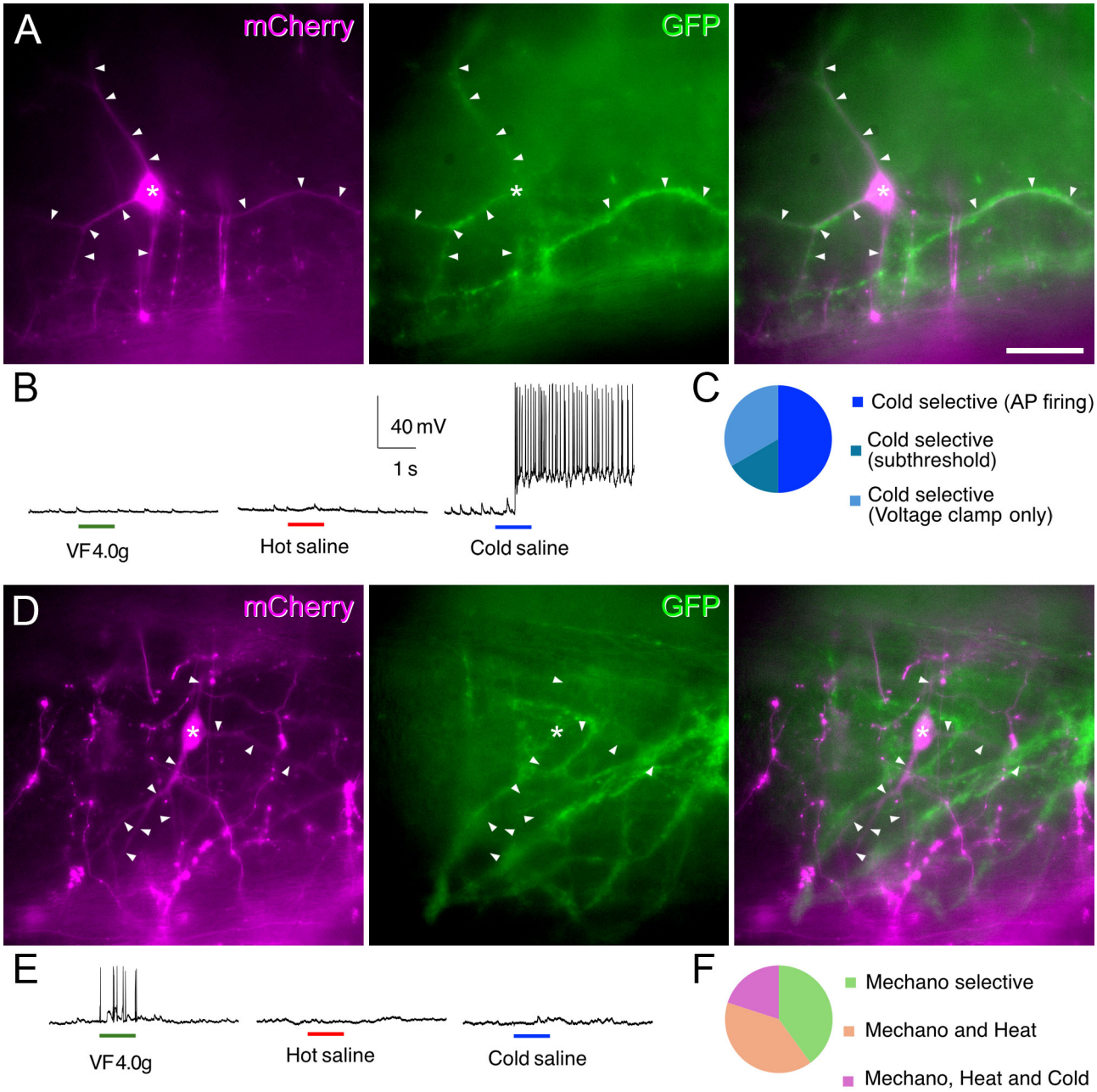

Figure 4. Electrophysiological characterisation of retrogradely labelled lamina I projection neurons recorded in Trpm8^{Flp};RCE:FRT mice (**A**) Fluorescence microscopy image of a retrogradely labelled (mCherry-positive) lamina I ALS neuron (soma marked with asterisk) that is densely coated by Trpm8-expressing (GFP-positive) axons. Note that bundles of GFP axons are closely associated with the dendrites of the retrogradely labelled neuron, which are marked with arrowheads. (**B**) Whole-cell recording from this cell reveals that only cold stimulation evoked action potentials (APs). (**C**) Pie chart showing the response properties of the 6 lamina I ALS neurons that were densely coated with Trpm8 afferents to mechanical, cold and heat stimulation of the skin. All of these cells responded only to cold stimulation: 3 cells showed APs, 1 cell showed EPSPs but no APs

Click here to enter text.

1066 (subthreshold), while 2 cells were recorded in voltage clamp and showed EPSCs. (**D**)
1067 Fluorescence microscopy image of a lamina I ALS neuron that was not densely coated
1068 with Trpm8 axons. Again, the soma is marked with an asterisk and dendrites with
1069 arrowheads. Note that although the dendrites of this cell pass through bundles of GFP
1070 axons these bundles are not aligned with the dendrites. (**E**) Whole-cell recording from the
1071 cell shown in (**D**). AP firing was evoked by mechanical stimulation (von Frey filament 4.0g),
1072 but not by application of hot or cold saline to the skin. (**F**) Pie chart of response properties
1073 of 5 lamina I ALS neurons that lacked dense Trpm8 input to mechanical, cold and heat
1074 stimulation to the skin. Two cells were mechano-selective, while three were polymodal (2
1075 cells: mechano, heat, 1 cell: mechano, heat and cold). Scale bar (**A**,**D**) = 50 μm. Scale
1076 bars in **B** apply to **E**.
1077

1078

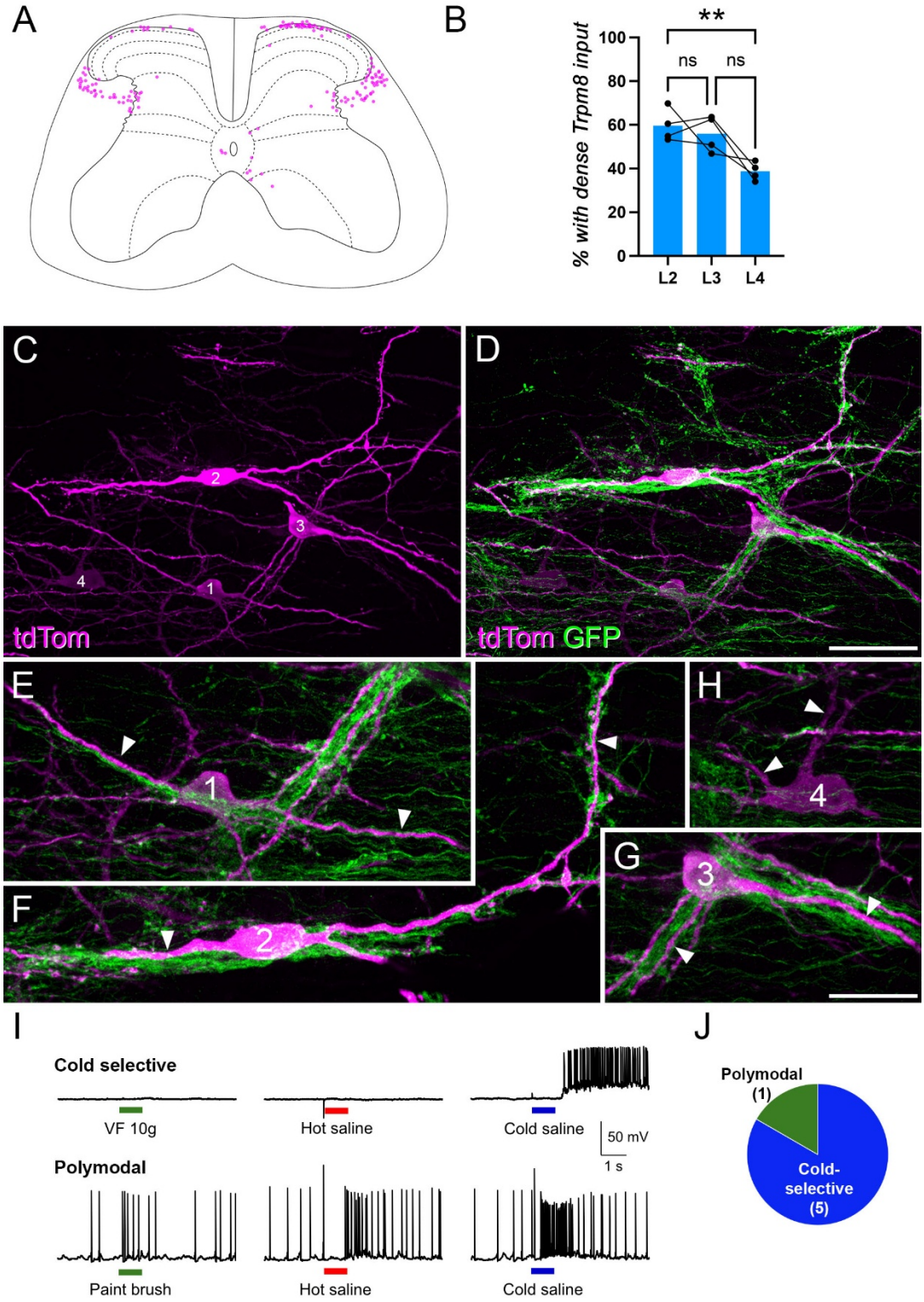

1079

1080 **Figure 5 Characterisation of Calb1-expressing projection neurons.** (**A**) The
1081 distribution of retrogradely labelled cells in 10 transverse sections from the L5 segment of
1082 one of the Calb1^{Cre} mice that had received an injection of AAV11.Cre^{ON}.tdTomato into the
1083 LPB. The right side of the plot is the side contralateral to the brain injection. (**B**) Bar chart

showing the proportion of retrogradely labelled cells in the L2, L3 and L4 segments of the Calb1^{Cre} mice injected with AAV11.Cre^{ON}.tdTomato into the LPB that received dense Trpm8 input. Repeated measures 1-way ANOVA showed a significant difference ($p = 0.048$), and post-hoc Holm-Šídák's multiple comparisons test revealed a difference only between L2 and L4 ($p = 0.0056$). (**C**) Part of a horizontal section through the L2 segment of one of the mice, showing 4 lamina I neurons (numbered 1-4) that were retrogradely labelled with tdTomato (tdTom, magenta). (**D**) The same field scanned to reveal both tdTomato and GFP (green). (**E**-**H**) detailed views of the 4 cells shown in **C**,**D**. Three of these cells (1-3) have numerous contacts from GFP-labelled axons on their dendrites (marked with arrowheads) and cell bodies. The fourth cell (4) has very few such contacts. (**I**) Recordings from one of the cold-selective cells (upper traces) and the polymodal cell (lower traces) in experiments carried out in Calb1^{Cre} mice that had received injections of AAV11.Cre^{ON}.tdTomato into the CVLM. The cell in the upper traces shows action potential firing in response to application of cold saline to the skin, but no response to application of a 10g von Frey (VF) hair or hot saline. The other cell responds to brushing of the skin with a paint brush, as well as to application of hot and cold saline. (**J**) Pie chart showing response characteristics of the 6 cells recorded in these experiments. Scale bars: (**C**,**D**) = 50 μm, (**E**-**H**) = 25 μm. **P<0.01.

Click here to enter text.

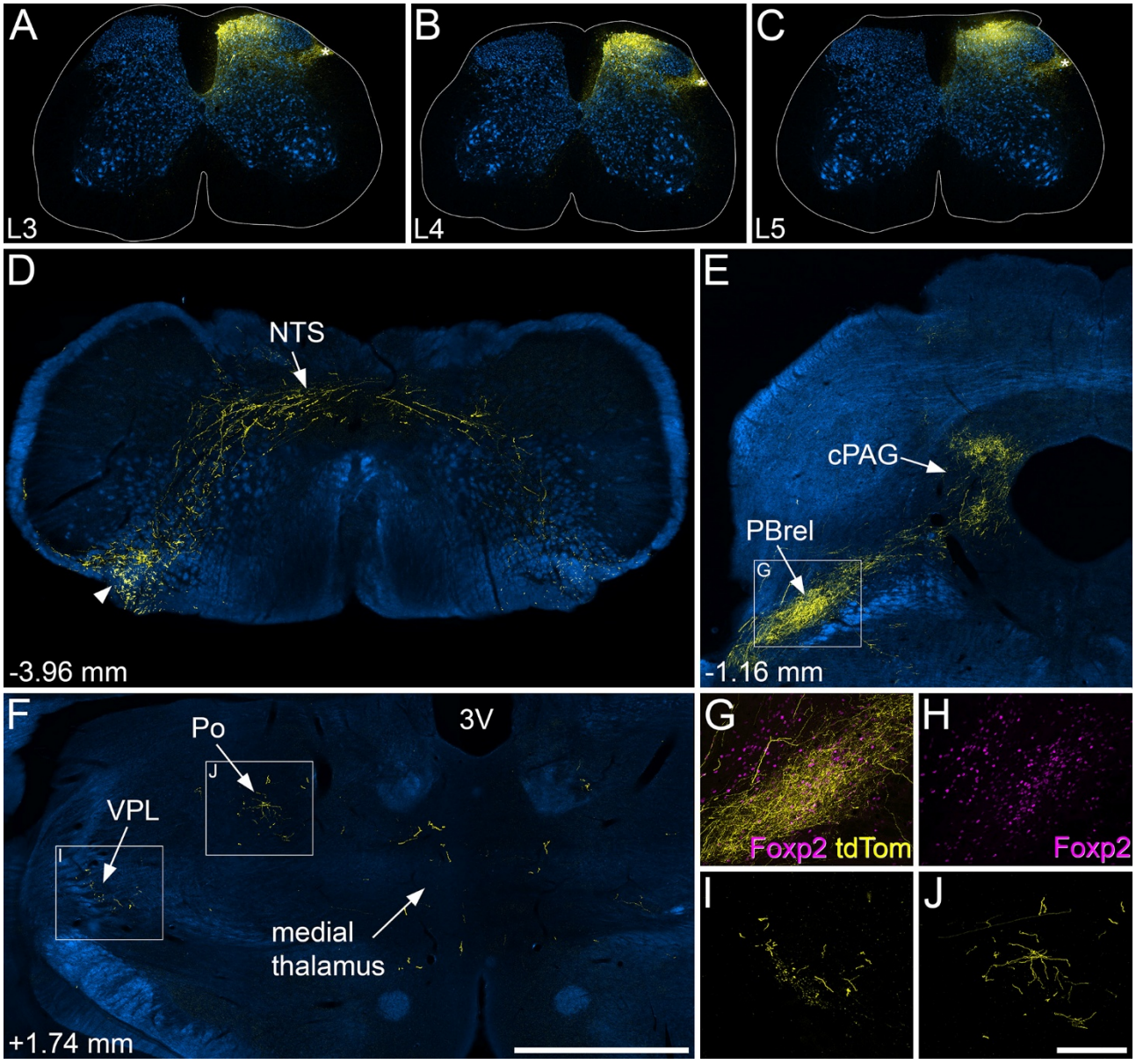

Figure 6. Anterograde tracing following injections of AAV1.Cre^{ON}.tdTomato into the medial dorsal horn of Calb1^{Cre} mice (**A**-**C**) Injection sites in the medial parts of the L3, L4 and L5 segments of one of the mice used in this part of the study. Immunostaining for tdTomato is shown in yellow and for NeuN in blue. Labelling of cell bodies is largely restricted to the medial part of the dorsal horn. There is some labelling in the lateral spinal nucleus (LSN), marked by asterisks, but this is likely to result from transport in axons of local interneurons. (**D**-**F**) Sections through selected regions of the brain immunostained to reveal tdTomato (yellow), with the corresponding dark-field images shown in blue. (**D**) At the level of the caudal medulla, the main ascending fibre bundle (arrowhead) lies in the ventrolateral region on the side contralateral to the spinal injections. Collateral axons innervate the nucleus of the solitary tract (NTS). (**E**) There is a dense projection of axons

to the rostralmost part of the lateral parabrachial area (PBrel) and the caudal part of the PAG (cPAG) on the side contralateral to the injections. (**F**) Within the diencephalon there is sparse labelling in the contralateral ventral posterolateral nucleus (VPL) and posterior nucleus (Po) as well as within the medial thalamus. (**G**,**H**) The region indicated in the box in **E** is shown at higher magnification with immunostaining for Foxp2 shown in magenta. The overlap between arborisation of tdTomato and Foxp2-positive nuclei indicates that this region is indeed PBrel. (**I**, **J**) show higher magnification views of tdTomato-positive axons in the VPL and Po, respectively, corresponding to the boxes in (**F**). Numbers in **D**-**F** show approximate rostrocaudal locations in relation to the interaural line. Images in **A**-**E**, **G**-**H** are from animal #8, and those in **F**, **I**, **J** are from animal #7 in Table 1. Scale bars: (**A**-**F**) = 1 mm, (**G**-**J**) = 200 μm.

Click here to enter text.

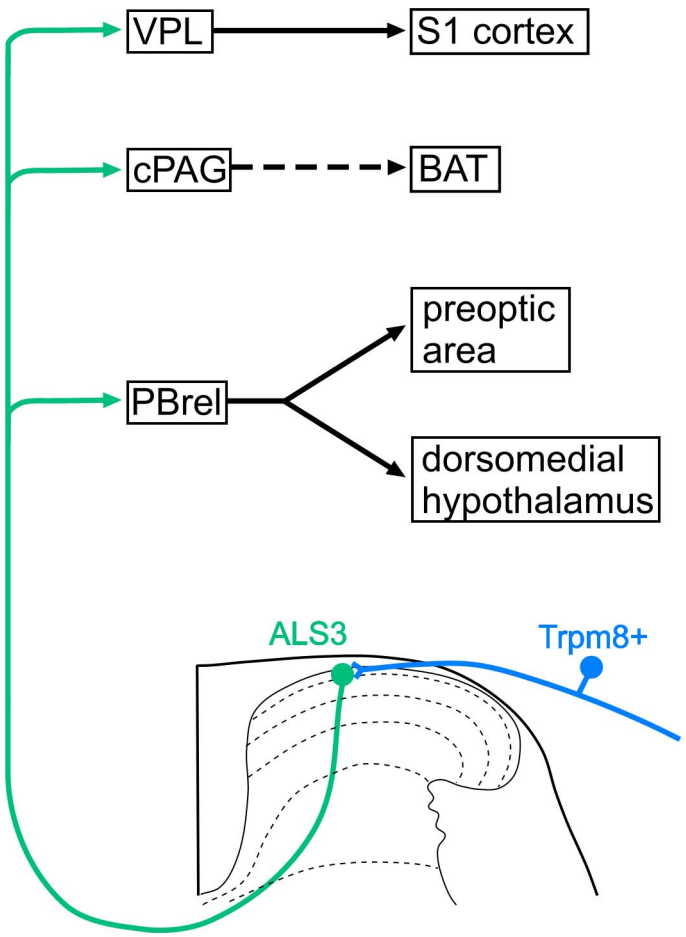

1127

1128

1129 **Figure 7. Proposed circuits involving cold-selective lamina I ALS neurons** Our results
1130 suggest that cold-selective lamina I projection neurons, which belong to the ALS3 cluster[9]
1131 project, among other sites, to PBrel, the caudal part of the PAG (cPAG) and the ventral
1132 posterolateral nucleus of the thalamus (VPL). Cold-responsive cells in PBrel innervate the
1133 preoptic area and dorsomedial hypothalamus, which are integral components of circuits
1134 that underlie cold defence. The cPAG can indirectly activate brown adipose tissue (BAT)
1135 metabolism, also contributing to cold defence. The projection to VPL, through its
1136 connection to the primary somatosensory cortex (S1), presumably underlies conscious
1137 perception of cold stimuli applied to the skin.

1138

Click here to enter text.

1139 **FIGURE SUPPLEMENTS**

1140

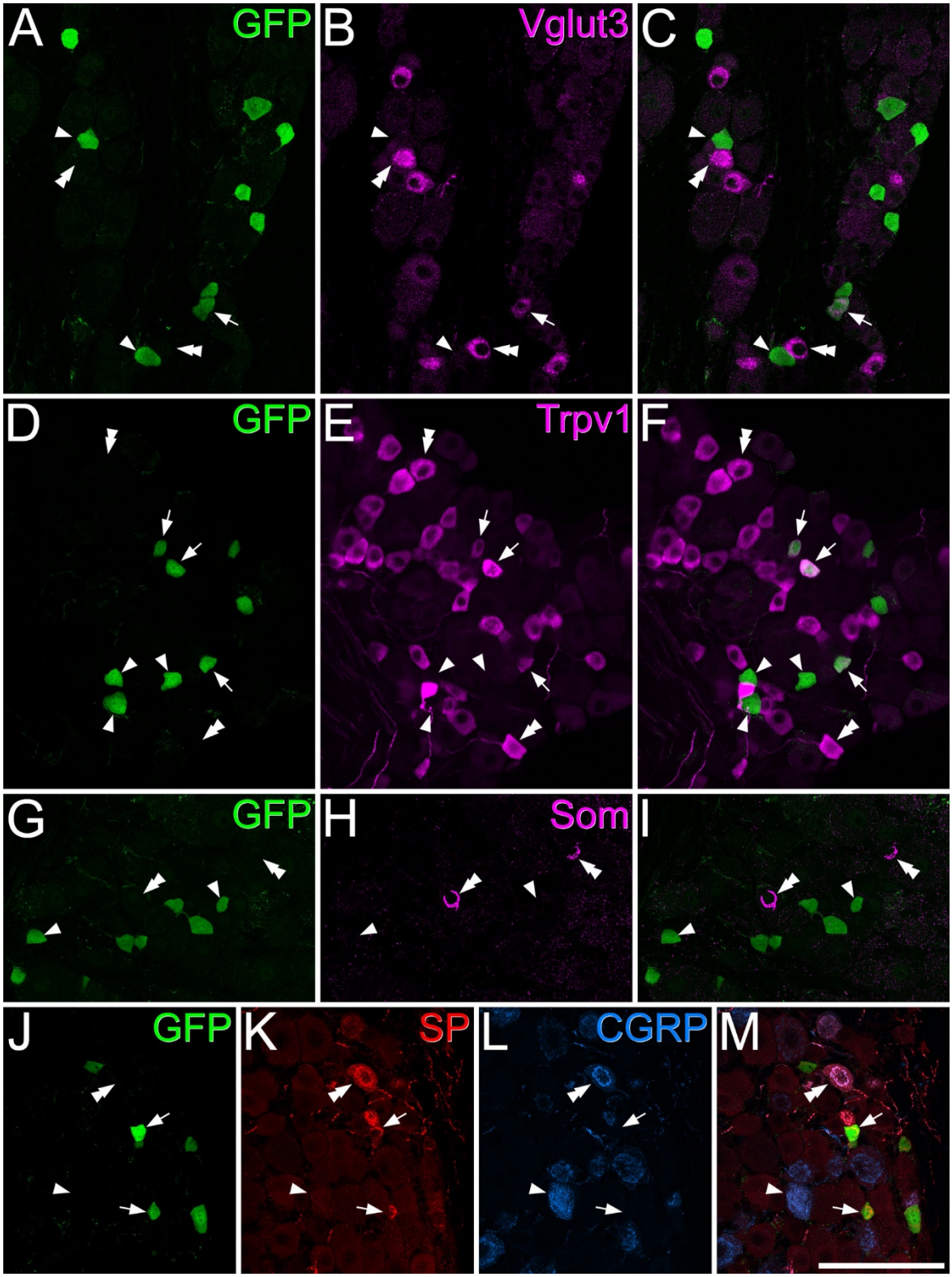

1141

1142 **Figure 1–figure supplement 1. Immunohistochemical characterisation of GFP-**
1143 **expressing somata in dorsal root ganglia of Trpm8^{Flp};RCE:FRT mice.** In each set of
1144 images GFP immunoreactivity is shown in green and other types of immunoreactivity in

magenta, red or blue. (**A**-**C**) GFP and Vglut3 are present in largely separate populations, although some cells contain both proteins (one cell in this field, marked with an arrow). Two cells containing only GFP are indicated with arrowheads, and two cells containing only Vglut3 with double arrowheads. (**D**-**F**) There is a greater degree of overlap between GFP and Trpv1, and three double-labelled cells are shown with arrows. Some cells with only GFP or Trpv1 are indicated with single and double arrowheads, respectively. (**G**-**I**) GFP and somatostatin (Som) are found in separate populations, and some labelled cells are marked with single and double arrowheads, respectively. Note that somatostatin is seen as a partial ring around the nucleus in cells that express the peptide. (**J**-**M**) GFP cells often contain substance P (SP) but lack calcitonin gene-related peptide (CGRP), and 2 of these are marked with arrows. A single and double arrowhead mark cells with CGRP only and with both SP and CGRP, respectively. Scale bar: (**A**-**M**) = 100 μm.

Click here to enter text.

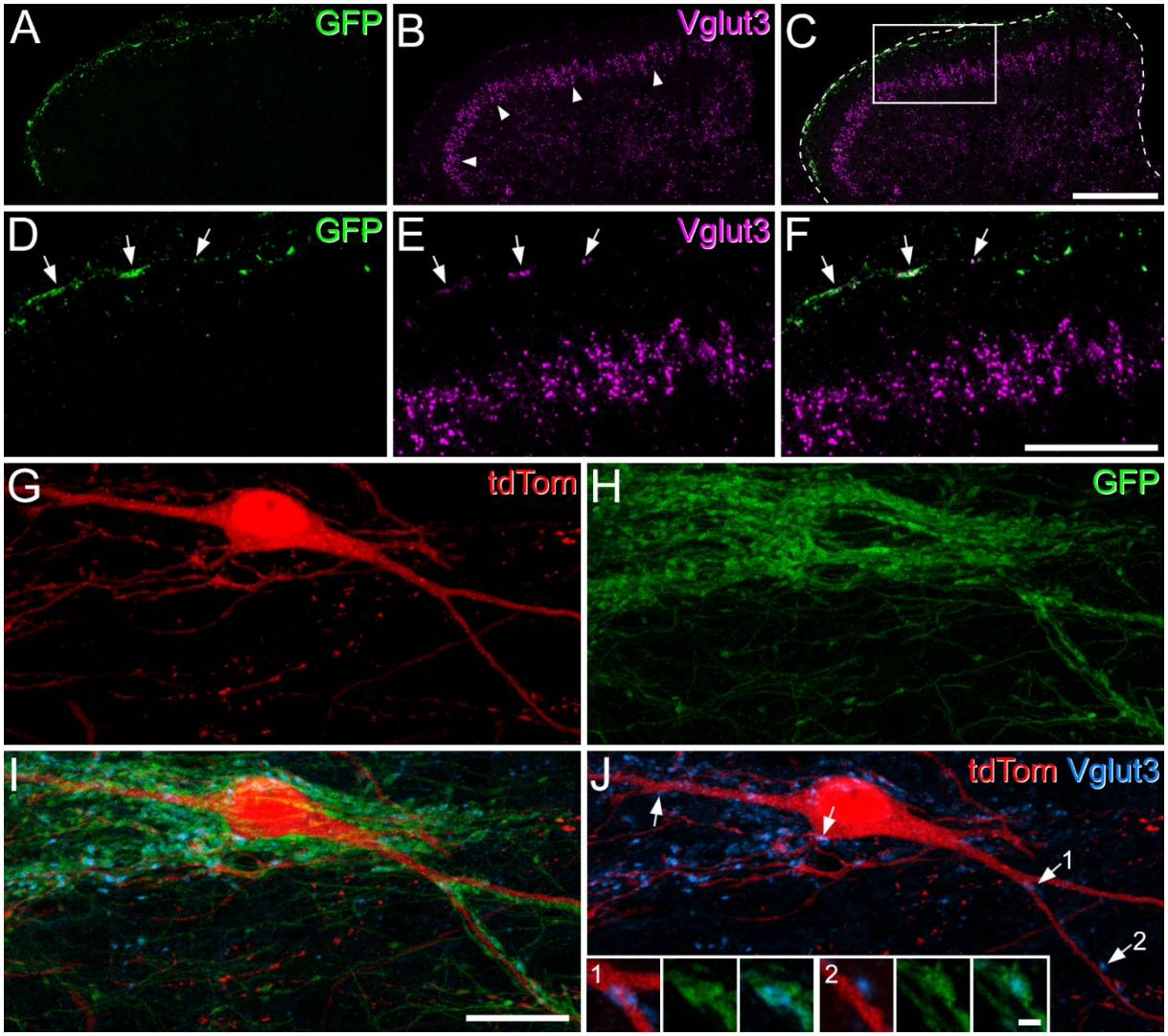

Figure 2–figure supplement 1. Expression of Vglut3 in the central terminals of Trpm8 afferents. (**A-C**) A low magnification confocal image from a transverse section of the L2 segment in a Trpm8^{Flp};RCE:FRT mouse immunostained for GFP (green) and Vglut3 (magenta). GFP-labelled axons are restricted to lamina I, while a dense band of Vglut3-immunoreactive terminals in the inner part of lamina II (marked with arrowheads) corresponds to the central terminals of C low-threshold mechanoreceptors. The dashed line in C shows the outline of the dorsal horn and the box indicates the area shown in (**D-F**). (**D-F**) At higher magnification a few Vglut3 profiles are also seen in lamina I (arrows) and these co-express GFP. (**G-J**) A horizontal section through lamina I from a Phox2a::Cre;Ai9;Trpm8^{Flp};RCE:FRT mouse immunostained to reveal tdTomato (tdTom, red), GFP (green) and Vglut3 (blue). This field includes a tdTomato labelled projection neuron that receives numerous contacts from GFP-labelled axons. Some of these are also immunoreactive for Vglut3 and these are seen more clearly (some marked with arrows) when only tdTomato and Vglut3 are revealed (**J**). The insets in J show two of these Vglut3

profiles (those marked with arrows numbered 1 and 2) contacting dendrites of the projection neuron in limited z-projections (2 optical sections at 0.5 μm z-spacing). In these images the coexpression of Vglut3 (blue) and GFP (green) is clearly visible. Scale bars: (**A**-**C**) = 100 μm, (**D**-**F**) = 50 μm, (**G**-**J**) = 50 μm, (insets in **J**) = 2 μm.

Click here to enter text.

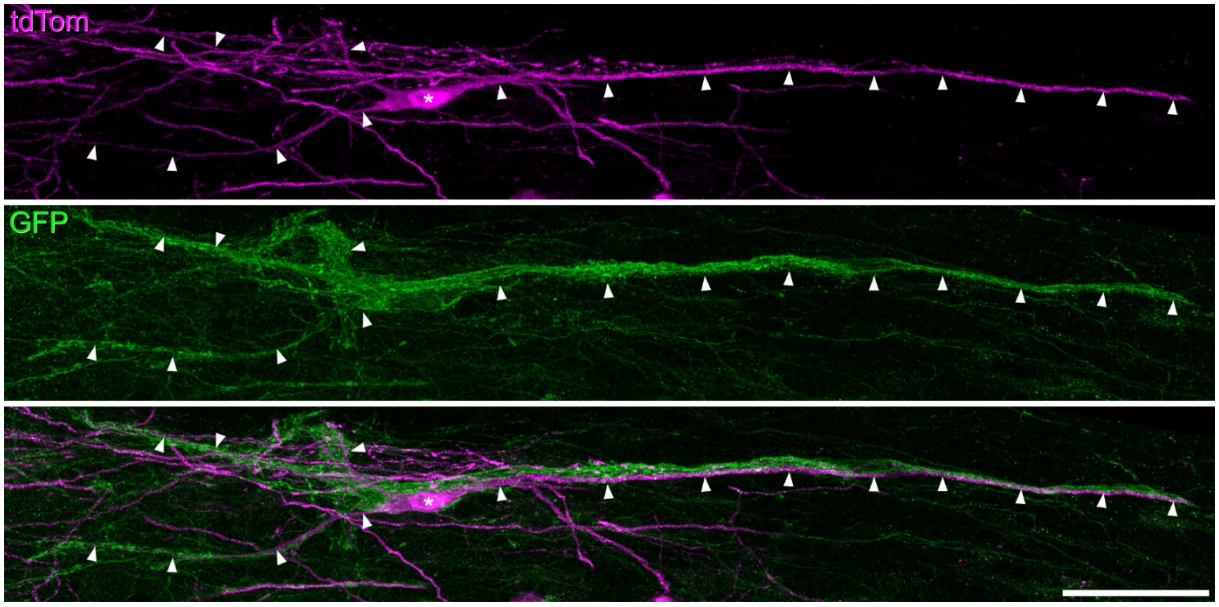

Figure 3–figure supplement 1. The relationship between tdTomato and GFP labelling for the cell illustrated in Figure 3. The top pane shows immunostaining for tdTomato (tdTom, magenta) in a horizontal section through lamina I from a Phox2a::Cre;Ai9;Trpm8^{Flp};RCE:FRT mouse. The tdTomato-labelled projection neuron illustrated in Figure 3 is visible. The soma is marked with an asterisk and parts of the dendritic tree with arrowheads. The cell body and dendrites are associated with dense bundles of GFP-labelled axons. Scale bar = 50 μm.

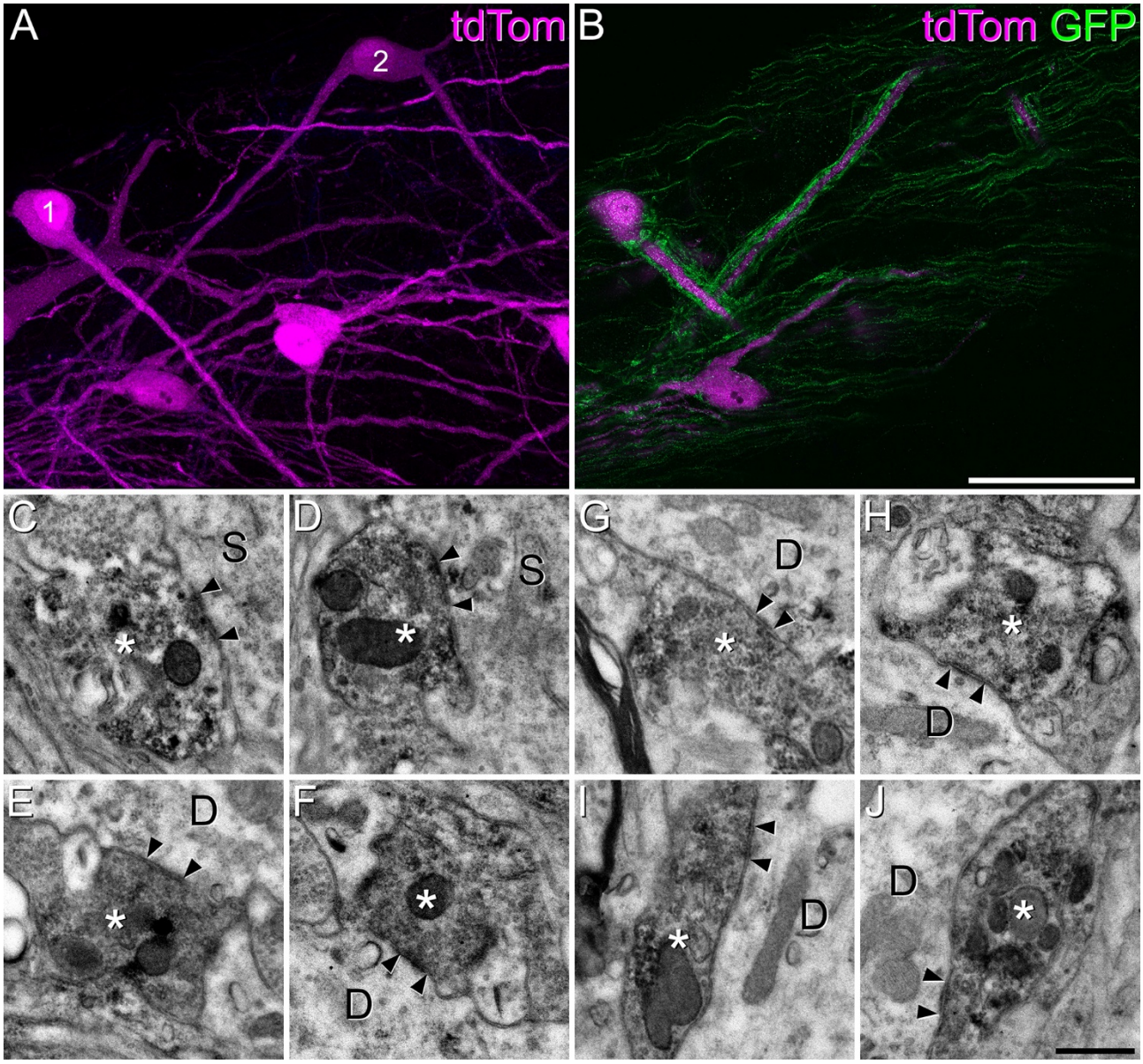

Figure 3–figure supplement 2. Confocal and electron microscope images of two Trpm8-innervated cells examined with the combined method in spinal cord sections from a Phox2a::Cre;Ai9;Trpm8^{Flp};RCE:FRT mouse. (**A**) Projected confocal z-stack showing parts of the two cells (numbered 1, 2) labelled with tdTomato (magenta) in a horizontal section. (**B**) a single optical section from the same confocal z-stack showing the association between axons labelled with GFP (green) and the cell body of cell 1 and dendrites of both cells. (**C-J**) Examples of synapses between the GFP-containing boutons, which are labelled with an immunoperoxidase method, and (unlabelled) dendrites (D) or soma (S) of the tdTomato-positive projection neurons. **C-F** show synapses on cell 1, and **G-J** those on cell 2. Presumed synaptic active zones (marked by arrowheads) can be recognised by the presence of vesicles on the presynaptic side and darkening of the

1203 membrane. However, these synapses do not show prominent postsynaptic densities.

1204 Scale bars: (**A**,**B**) = 50 µm, (**C**-**J**) = 500 nm.

Click here to enter text.

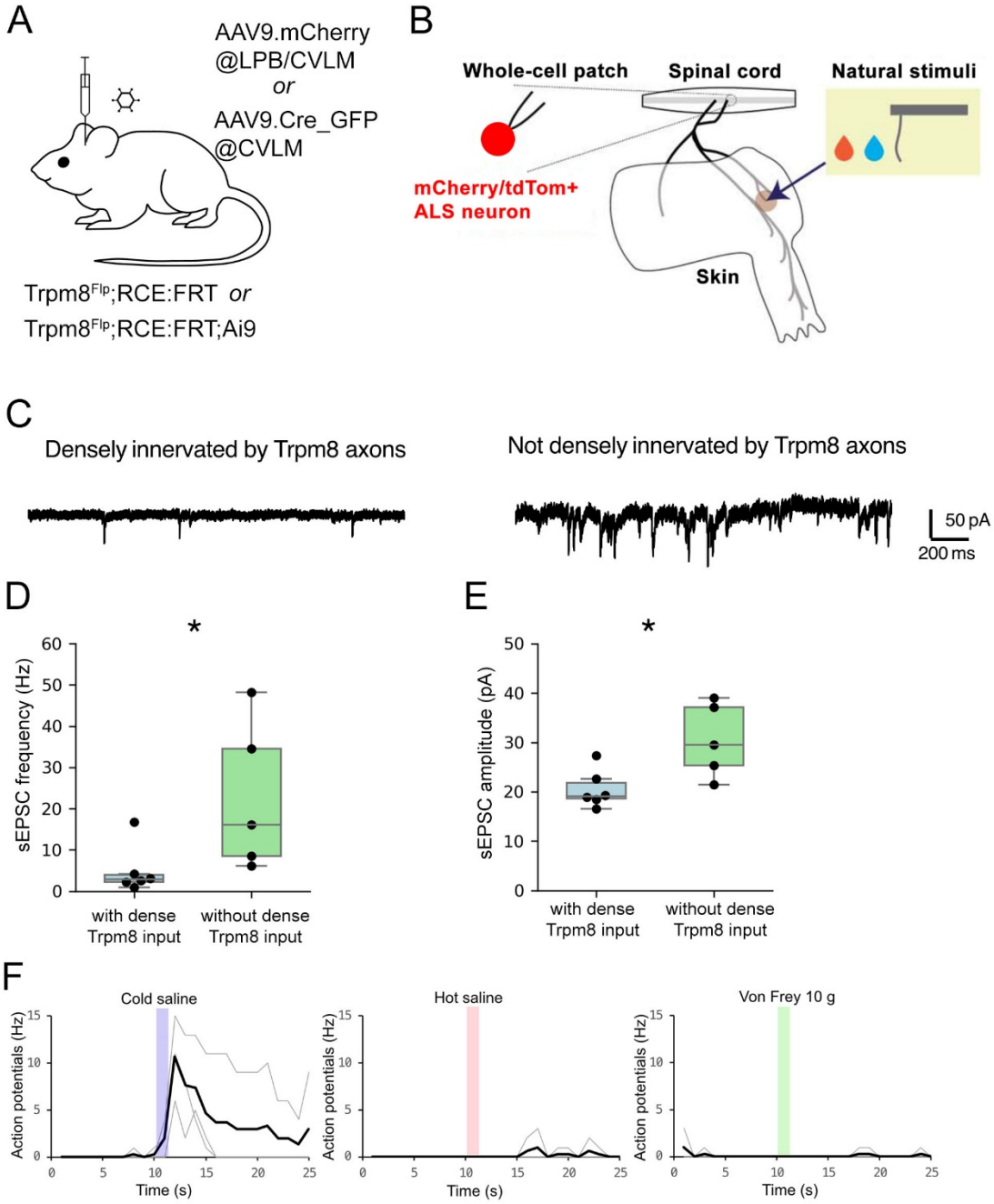

Figure 4–Figure supplement 1. Recording strategy and characteristics of spontaneous EPSCs in cold-selective and other lamina I ALS cells. (**A**) Cells were identified by expression of mCherry following injection of AAV9.mCherry into the CVLM or LPB of Trpm8^{Flp};RCE:FRT mice, or by expression of tdTomato following injection of AAV9.Cre_GFP into the CVLM of Trpm8^{Flp};RCE:FRT;Ai9 mice. Note that the level of GFP expression resulting from injection of AAV9.Cre_GFP was extremely low, and would have been restricted to the nucleus of labelled neurons, due to the presence of a nuclear localisation signal. In both cases, Trpm8-expressing afferents were labelled with GFP. (**B**) The semi-intact somatosensory preparation retained skin attached to lumbar spinal cord

through intact peripheral nerves and was used for recording responses to natural skin stimuli. (**C**) Representative traces from an ALS neuron with dense Trpm8 input (left) and an ALS neuron without dense Trpm8 input (right). (**D**, **E**) Quantification of sEPSC frequency (**D**) and amplitude (**E**) of ALS neurons. Box plots are median and interquartile range with symbols representing data points from individual ALS neurons (with dense Trpm8 input: n=6, without dense Trpm8 input: n=5; * indicates $p < 0.05$, Mann-Whitney U test). (**F**) Overlay of the firing time course of 3 cold-selective cells in response to cold, heat and mechanical stimulation. Individual traces shown in grey and averages in black.

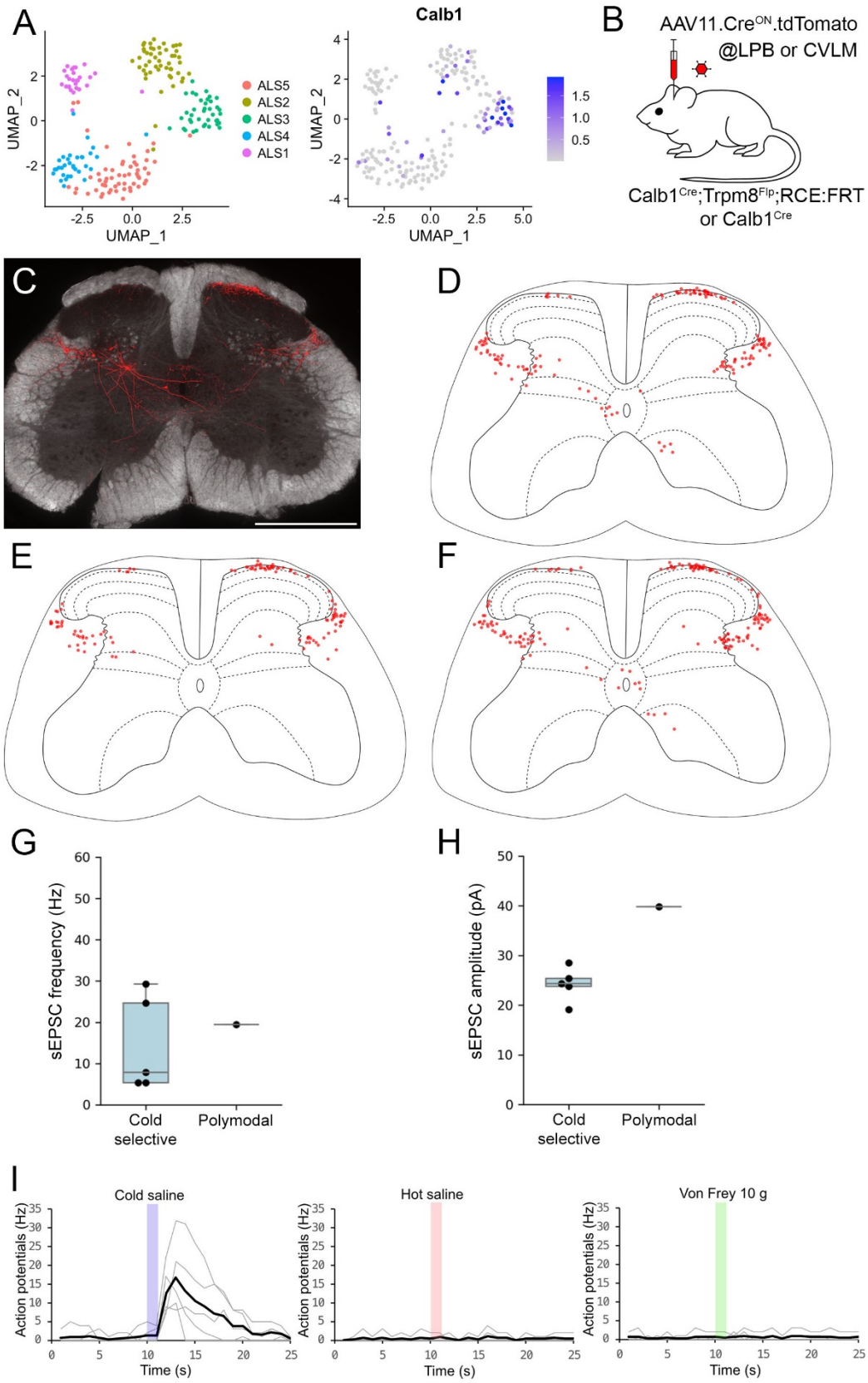

Figure 5–figure supplement 1. **Further characterisation of Calb1-expressing projection neurons.** (**A**) UMAP plot showing the distribution of cells in the ALS1-5 clusters, together with a plot for expression of Calb1. Note the presence of many Calb1-positive cells in the ALS3 cluster. (**B**) The experimental approach used to generate data

Click here to enter text.

presented in this figure and in Figure 5. (**C**) An example of a section through the L5 segment from a Calb1^{Cre} mouse injected with AAV11.Cre^{ON}.tdTomato in the LPB. Expression of tdTomato (red) is superimposed on a dark field image. (**D**-**F**) The distribution of retrogradely labelled cells in 9 (**D**,**F**) or 8 (**E**) transverse sections from the L5 segments of the remaining 3 Calb1^{Cre} mice injected with AAV11.Cre^{ON}.tdTomato in the LPB. The labelling for the other mouse is shown in Figure 5A. (**G**, **H**) sEPSC frequencies and amplitudes for the 5 cold-selective cells and the 1 polymodal cell recorded in Calb1^{Cre} mice injected with AAV11.Cre^{ON}.tdTomato in the CVLM. Note that although 2 of the cold-selective cells in this sample had relatively high sEPSC frequencies, when data from these cells were pooled with those reported for other sample of cold-selective cells (shown in Figure 4–Figure supplement 1) and compared with the polymodal cells shown in that Figure supplement, there was still a significant difference for both sEPSC frequency ($p = 0.037$) and amplitude ($p = 0.015$) (Mann-Whitney U test). (**I**) Overlay of the firing time course of 5 cold-selective cells in response to cold, heat and mechanical stimulation. Individual traces shown in grey and averages in black. Scale bar: (**C**) = 500 μm.

Click here to enter text.

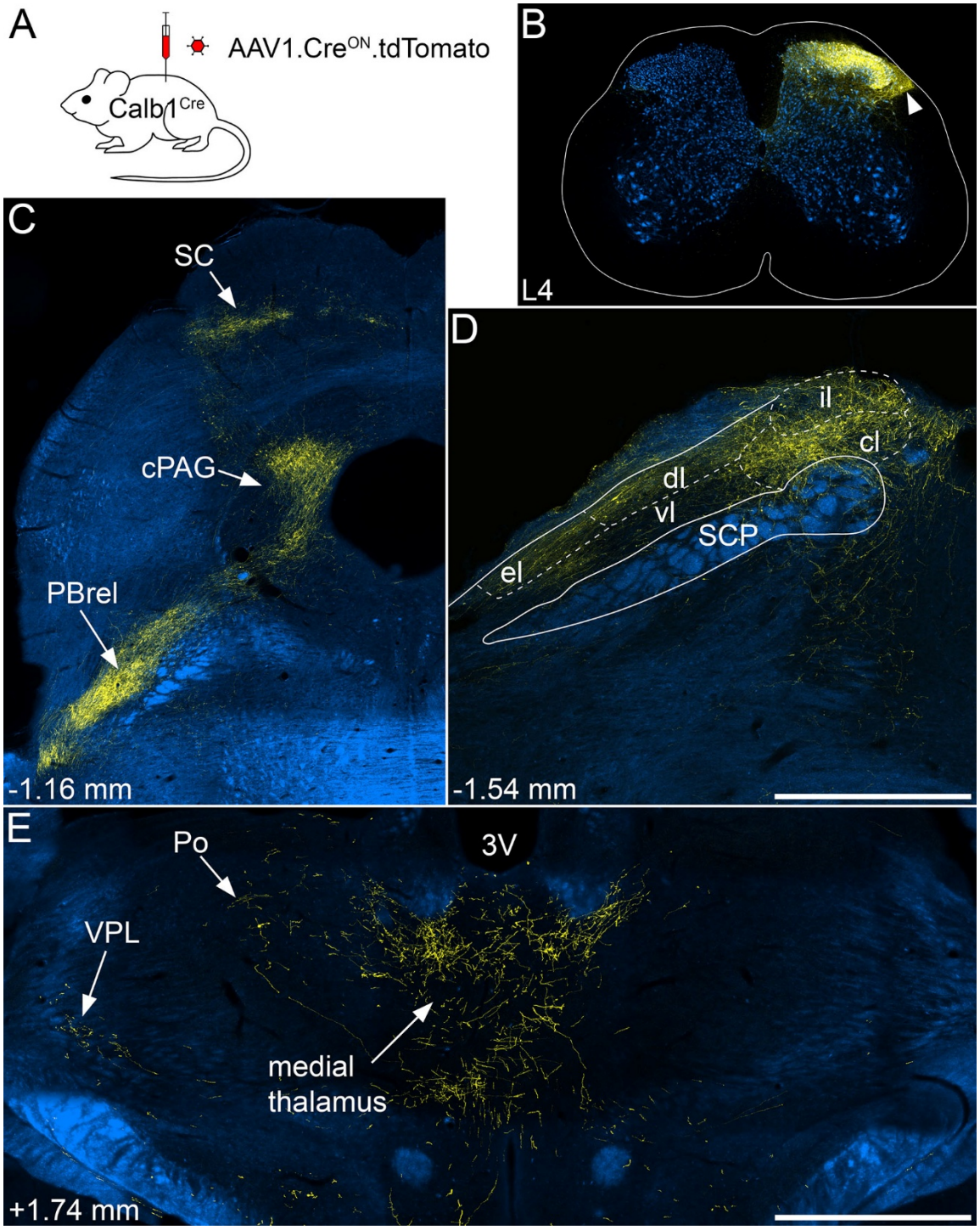

Figure 6–figure supplement 1. Anterograde labelling following injections of AAV1.Cre^{ON}.tdTomato into the central part of the spinal dorsal horn of Calb1^{Cre} mice. (**A**) The experimental approach used to generate data for Figure 6 and for Figure 6–figure supplements 1-3. Intraspinal injections were made into either the L3 or the L3, L4 and L5 segments, and were targeted on either the central or medial part of the dorsal horn. (**B**) Example of an injection into the central part of the L4 segment of a Calb1^{Cre} mouse. Immunostaining for tdTomato is shown in yellow and for NeuN in blue. There is extensive

tdTomato labelling throughout most of the dorsal horn, and this extends into the lateral spinal nucleus (arrowhead), which contains tdTomato-labelled cell bodies. (**C**-**E**) Sections through selected regions of the brain have been immunostained to reveal tdTomato (yellow), and these are shown on corresponding dark-field images (blue). (**C**) There is strong labelling in the rostralmost part of the contralateral LPB, corresponding to the PBrel, as well as in the caudal PAG (cPAG). Unlike the pattern seen with injections restricted to the medial dorsal horn, there is also strong labelling in the contralateral superior colliculus (SC). (**D**) At a slightly more caudal level there is axonal labelling in several subnuclei of the contralateral LPB, including external lateral (el), dorsolateral (dl), central lateral (cl) and internal lateral (il), but not ventrolateral (vl). The location of the superior cerebellar peduncle (SCP) is indicated. (**E**) Within the diencephalon there is sparse axonal labelling in contralateral VPL and posterior (Po) thalamic nuclei, as seen following medial injections. However, there is also dense labelling in the medial thalamus, which was not seen with medial injections. Numbers in **C**-**E** show approximate rostrocaudal locations in relation to the interaural line. All images are from animal #2 in Table 1. Scale bars: (**B**,**C**,**E**) = 1 mm, (**D**) = 500 μm.

Click here to enter text.

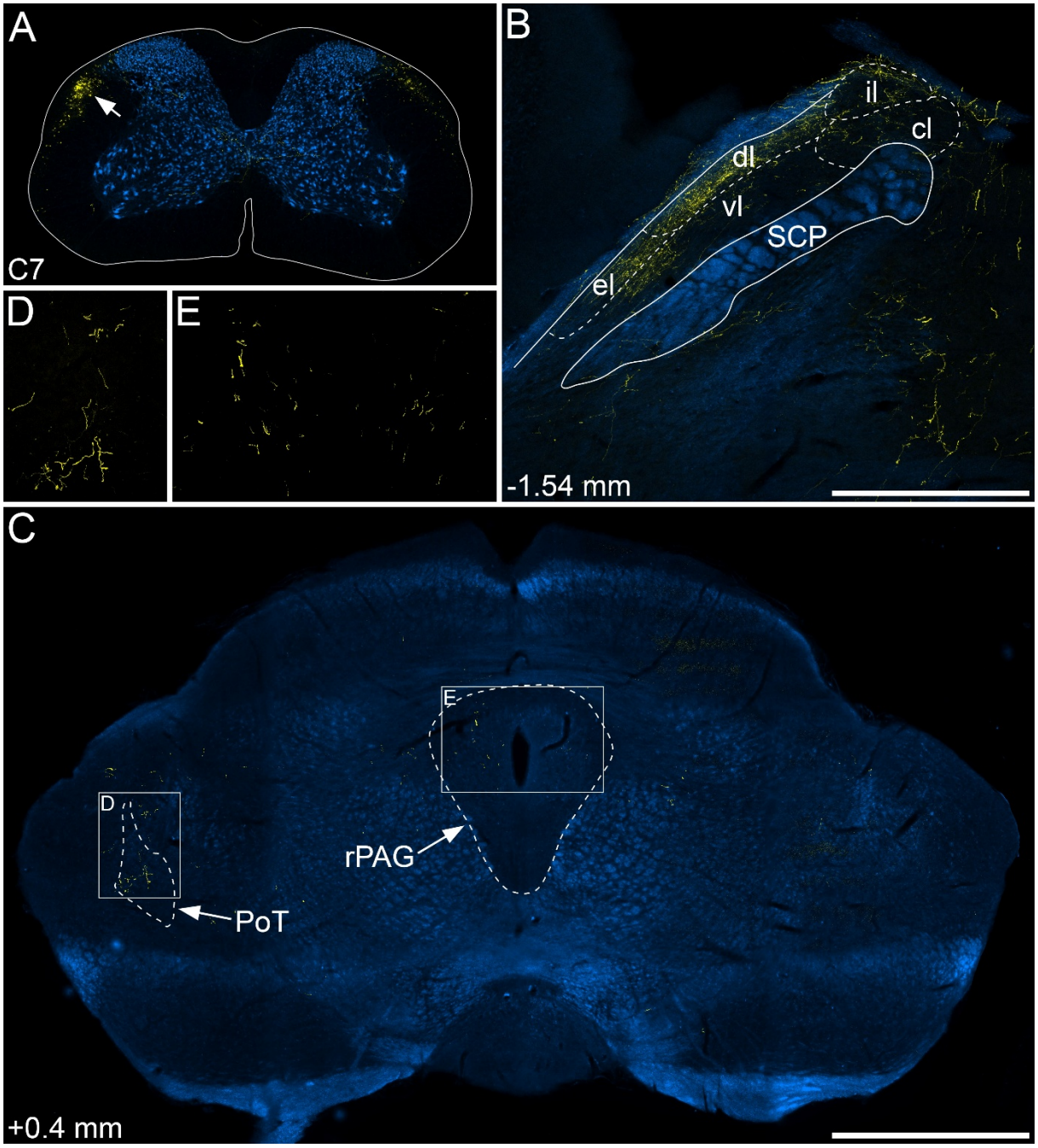

Figure 6–figure supplement 2. Anterograde labelling following injections of AAV.Cre^{ON}.tdTomato into the medial dorsal horn of Calb1^{Cre} mice. (**A**) A section through the C7 segment of a mouse that received injections into L3, L4 and L5 segments. Immunostaining for tdTomato is shown in yellow and for NeuN in blue. There is a bundle of axons (arrow) in the contralateral dorsolateral white matter, with a much more weakly stained bundle in the same location on the opposite side. A few collateral branches are present in the deep dorsal horn and the area around the central canal. (**B**,**C**) Sections through selected regions of the brain have been immunostained to reveal tdTomato (yellow), and this is shown on corresponding dark-field images (blue). (**B**) At this level of

the contralateral LPB, there is axonal labelling in the external lateral (el) and dorsolateral (dl) subnuclei, with very little labelling in ventrolateral (vl), central lateral (cl) or internal lateral (il). The location of the superior cerebellar peduncle (SCP) is indicated. (**C**) At a level corresponding to ~ 0.4 mm rostral to the interaural line there is very sparse axonal labelling in the posterior triangular nucleus of the thalamus (PoT) and in the rostral PAG (rPAG) on the side contralateral to the spinal injection. This is shown at higher magnification in (**D**) and (**E**), which correspond to the boxes in (**C**). Numbers in **B** and **C** show approximate rostrocaudal locations in relation to the interaural line. Images in **A** and **C**-**E** are from animal #7, and that in **B** from animal # 8 in Table 1. Scale bars: (**A**,**C**) = 1 mm, (**B**,**D**,**E**) = 500 μm.

Click here to enter text.

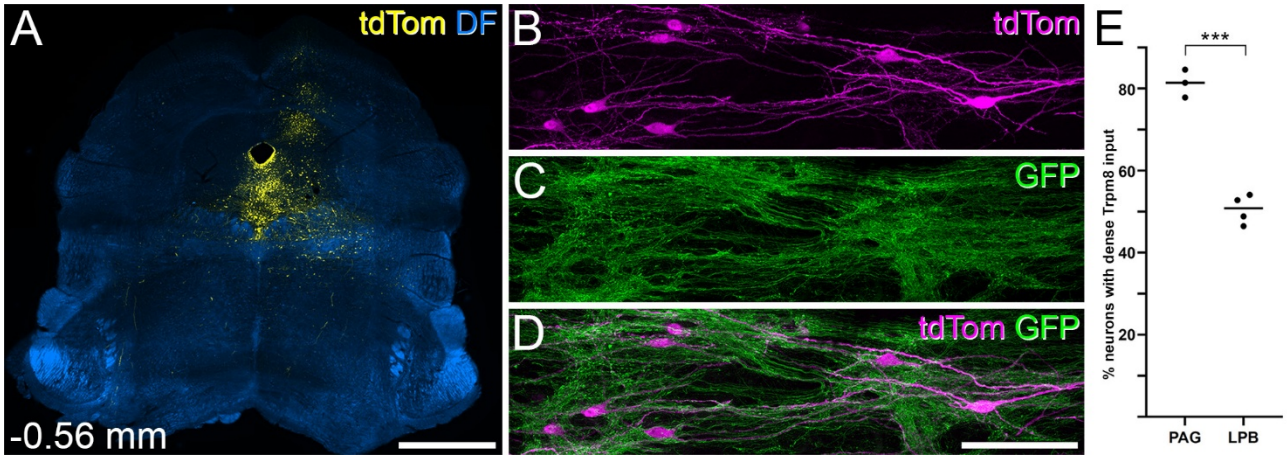

Figure 6–figure supplement 3. Retrograde labelling of Calb1-expressing ALS neurons from PAG. (**A**) TdTomato labelling at the site of injection of AAV11.Cre^{ON}.tdTomato in one of the 3 Calb1^{Cre};Trpm8^{Flp};RCE:FRT mice used in this part of the study. Note that this will not reveal the precise location of the injection, because only nearby Calb1-expressing cells will be labelled. (**B**-**D**) Labelling for tdTomato (tdTom) and GFP in a horizontal section through lamina I from the case illustrated in (**A**). Several tdTom-positive neurons are visible in this field, and all of them are densely coated with GFP-labelled (Trpm8-positive) axons. (**E**) Histogram showing the percentages of retrogradely labelled neurons in the L2-L4 segments that were densely coated with Trpm8-positive axons in this set of experiments (PAG), compared with the corresponding values from the 4 cases in which AAV11.Cre^{ON}.tdTomato was injected into the LPB. There was a highly significant difference between the percentages between the two injection sites ($p < 0.0001$, unpaired t-test with Welch's correction). Scale bars: (**A**) = 1 mm, (**B**-**D**) = 100 µm.

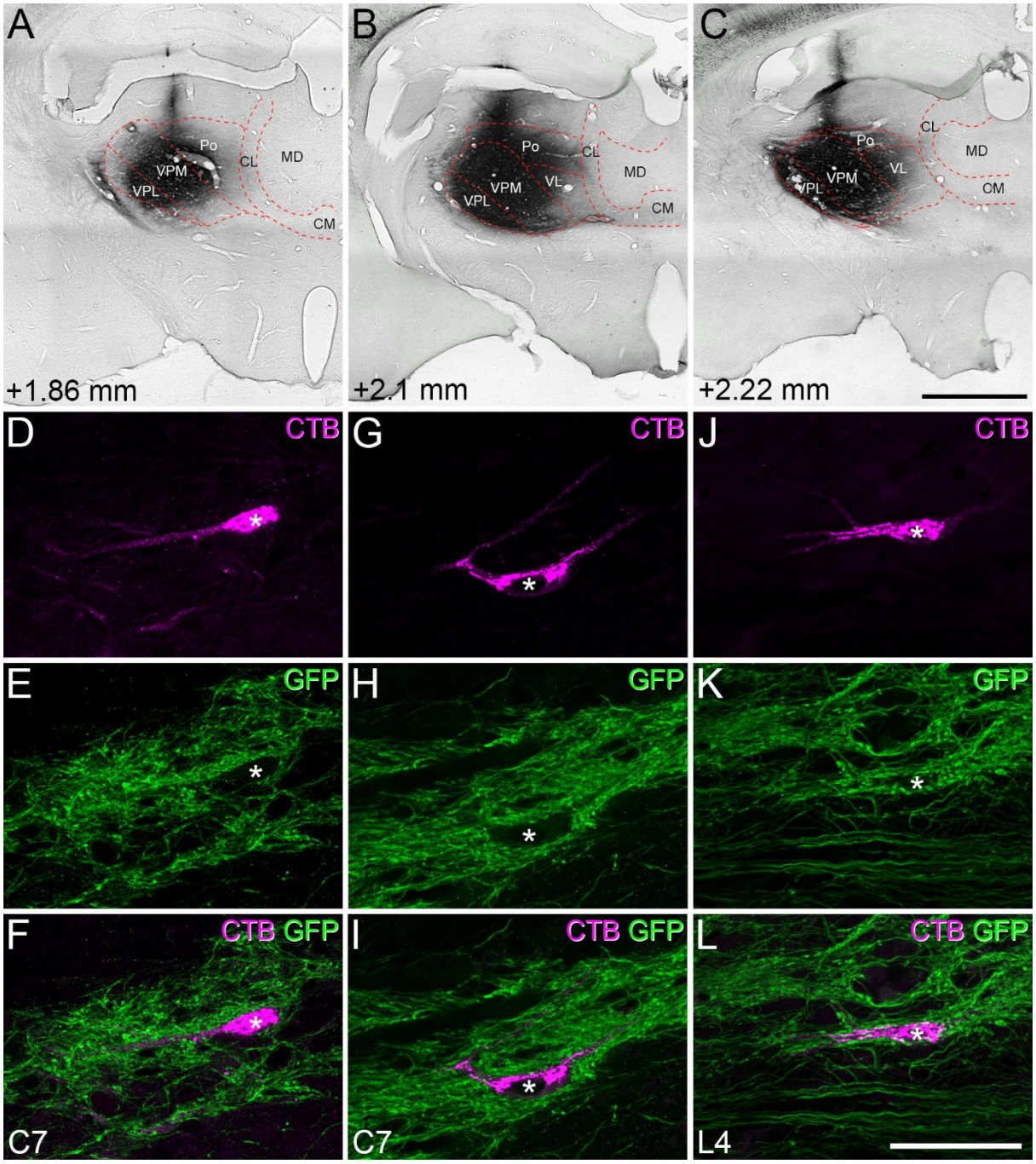

Figure 6–figure supplement 4. Identification of spinothalamic lamina I neurons with dense Trpm8 input. (**A**-**C**) CTB injection sites in the 3 experiments. In each case there is dense labelling in the ventral posterolateral (VPL) and ventral posteromedial (VPM) nuclei, together with some labelling in the posterior (Po) nucleus, and in two cases also in the ventrolateral (VL) nucleus. Note the lack of labelling in medial thalamic nuclei (centrolateral, CL; centromedial, CM; mediodorsal, MD). Numbers show approximate rostrocaudal locations in relation to the interaural line. (**D**-**I**) Examples of retrogradely labelled (CTB-positive) lamina I neurons (marked with asterisks) that are associated with numerous GFP-labelled (Trpm8-expressing) axons in horizontal sections through the C7

Click here to enter text.

segments in the experiments illustrated in **A** and **B**. (**J**-**L**) In the experiment illustrated in **C**, we also identified 5 CTB-labelled cells in the L4 segment, and one of these, which is associated with numerous GFP-labelled boutons, is shown here (asterisk). Note that we also found CTB-labelled cells associated with numerous GFP-positive boutons in the C7 segment in this experiment. In each case, the images are shown below the injection site from the corresponding experiment. Scale bars: (**A**-**C**) = 1 mm, (**D**-**L**) = 50 μm.

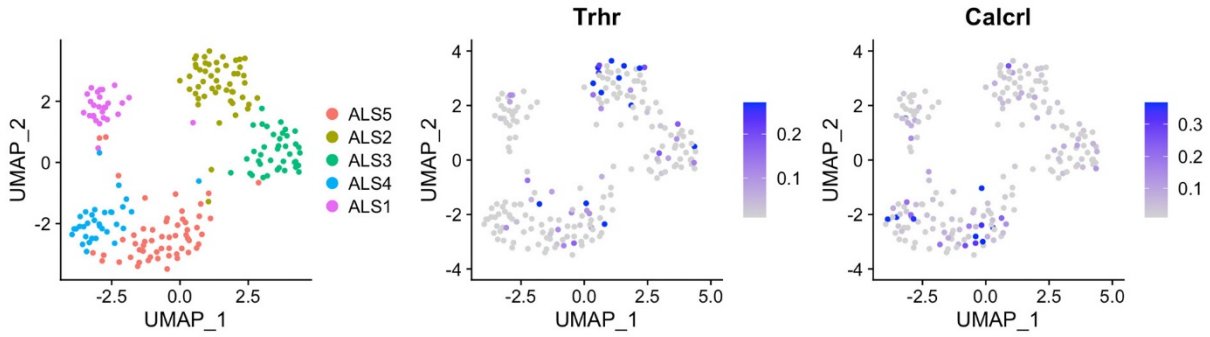

Figure 7–Figure supplement 1 UMAP plot showing the distribution of cells in the ALS1-5 clusters, together with plots for expression of Trhr and Calcrl. Note the presence of both Trhr and Calcrl in several of the ALS clusters, including ALS3.

1327 Table 1 Experimental details for Calb1^{Cre} mice used in anterograde tracing experiments.

1328

Animal	Sex	Injected segments	Injection location	Injection volume (nl)	Viral load (GC)	Survival (days)
1	M	L3, L4, L5	central	300	9.48×10^7	26
2	M	L3, L4, L5	central	300	9.48×10^7	55
3	F	L3, L4, L5	central	300	9.48×10^7	57
4	M	L3	central	300	9.48×10^7	42
5	F	L3	central	300	9.48×10^7	40
6	F	L3	central	300	9.48×10^7	40
7	M	L3, L4, L5	medial	150	4.74×10^7	55
8	M	L3, L4, L5	medial	150	4.74×10^7	54
9	F	L3, L4, L5	medial	150	4.74×10^7	41
10	F	L3	medial	150	4.74×10^7	41
11	F	L3	medial	150	4.74×10^7	41
12	F	L3	medial	150	4.74×10^7	53

1329

1330 Mice received injections of AAV1.Cre^{ON}.tdTomato into either the L3 segment only, or into
1331 the L3, L4 and L5 segments on the right side. Injections were either targeted centrally (400
1332 µm lateral to the midline) or medially (250 µm lateral to the midline) within the dorsal horn.
1333 All injections were made at 300 µm below the surface of the spinal cord. Injection volume
1334 and viral load refer to each injection in animals 1-3 and 7-9.